Mid-latitude trans-Pacific reconstructions and comparisons of coupled glacial/interglacial climate cycles based on soil stratigraphy of cover-beds

B.V. Alloway [a, b, *], P.C. Almond [c], P.I. Moreno [d], E. Sagredo [e], M.R. Kaplan [f], P.W. Kubik [g], P.J. Tonkin [h]

[a] School of Environment, The University of Auckland, Private Bag 92019, Auckland, New Zealand
[b] Centre for Archaeological Science (CAS), School of Earth and Environmental Sciences, University of Wollongong, Wollongong, NSW, 2522, Australia
[c] Department of Soil and Physical Sciences, Faculty of Agriculture and Life Sciences, PO Box 8084, Lincoln University, Canterbury, New Zealand
[d] Instituto de Ecología y Biodiversidad, Departamento de Ciencias Ecológicas, Universidad de Chile, Casilla 653, Santiago, Chile
[e] Instituto de Geografía, Pontificia Universidad Católica de Chile, Av. Vicuna Mackenna, 4860, Santiago, Chile
[f] Lamont-Doherty Earth Observatory Columbia University, Palisades, NY, 10964-8000, United States
[g] Paul Scherrer Institut, c/o Institute of Particle Physics, HPK H30, ETH Hoenggerberg, CH-8093, Zurich, Switzerland
[h] 16 Rydal Street, Christchurch 8025, New Zealand

ARTICLE INFO

ABSTRACT

South Westland, New Zealand, and southern Chile, are two narrow continental corridors effectively confined between the Pacific Ocean in the west and high mountain ranges in the east which impart significant influence over regional climate, vegetation and soils. In both these southern mid-latitude regions, evidence for extensive and repeated glaciations during cold phases of the Quaternary is manifested by arrays of successively older glacial drift deposits with corresponding outwash plain remnants. In South Westland, these variably aged glacial landforms are mantled by layered (multisequal) soils characterised by slow loess accretion and pedogenesis in an extreme leaching and weathering environment. These cover-bed successions have undergone repeated coupled phases of topdown and upbuilding soil formation that have been related to fluctuating cycles of interglacial/warm and glacial/cold climate during the Quaternary. In this study, we recognise multisequal soils overlying glacial landforms in southern continental Chile but, unlike the spodic (podzolic) soil sequences of South Westland, these are of dominantly volcanigenic (andic) provenance and are very similar to multisequal soils of andic provenance that predominate in, and adjacent to, areas of rhyolitic to andesitic volcanism in North Island, New Zealand. Here we develop a soil-stratigraphic model to explain the observed occurrence of multisequal soils mantling dominantly glacial landforms of southern continental Chile. Based on proxy data from southern Chile, we propose that persistent vegetation cover and high precipitation on the western side of the Andes, during colder-than-present episodes tended to suppress the widespread production of glacially-derived loessial materials despite the pervasive occurrence of glacial and glacio-fluvial deposits that have frequently inundated large tracts of this landscape during the Quaternary. Given the lack of loess cover-beds that have traditionally assisted in the relative dating of glacial episodes prior to the Late Quaternary, surface exposure dating techniques could provide another chronological alternative to address this issue. However, there have been two main obstacles to successfully apply this dating technique in Patagonia. First, minimum exposure ages may be obtained on moraines older than the last glacial cycle due to erosion, although dating outwash plains is more robust. Second, on the wet western side adjacent to the Andes, persistent vegetation cover during both glacial and post-glacial times, as well as widespread inundation by volcanic mass-flows, appear preventive. We make a case that soil genesis within this region appears to be dominated by a constant flux of intermittently erupted Andean-sourced tephra which has continued to upbuild soils at the ground surface separated by intervals where topdown weathering processes are intensified. As already demonstrated by New Zealand studies, multisequal soil successions have a clear implied connection to coupled glacial and interglacial climate cycles of the

* Corresponding author. School of Environment, The University of Auckland, Private Bag 92019, Auckland, New Zealand.
E-mail address: brent.alloway@gmail.com (B.V. Alloway).

Quaternary. On this basis, similar sequences in northwest Patagonia provide a relatively untapped archive to enable Quaternary glacial and environmental changes in this pervasively glaciated volcanic region to be constructed.

1. Introduction

Southern continental Chile and South Westland, New Zealand, share similar southern mid-latitude positions within the southern westerly wind (SWW) belt and are located immediately westward of north-south trending high (>2000-m above sea level) mountain ranges that form significant topographic barriers influencing precipitation in these regions. At both locations, evidence for extensive and repeated glaciations during cold climate phases of the Quaternary is manifested in the landscape by an impressive array of glacial drift deposits with corresponding outwash plains.

In South Westland (~43°S), densely forested, fluvio-glacial landforms and associated soil cover-bed successions have been studied in detail (Almond, 1996; Almond and Tonkin, 1999; Almond et al., 2001) and this research has contributed to the formulation of a robust regional glacial chronostratigraphic framework (e.g. Nathan et al., 2002; Cox and Barrell, 2007). Across the Pacific Ocean and at similar southern latitude, the configuration and internal architecture of ice lobes in southern continental Chile (northwest Patagonia) is well-known based largely from seminal glacial morphologic maps (i.e. Caldenius, 1932; Andersen et al., 1999; Denton et al., 1999a,b). In contrast to the South Westland glaciated landscape, however, the soil cover-bed stratigraphies that mantle this glacial sequence have not been documented in any detail. The closest related studies are well to the south on the east arid side of the Andes (Douglass and Bockheim, 2006). In our study, we identify the first occurrence of multisequal soils mantling these glacial landforms in southern continental Chile, and develop a soil-stratigraphic model based on soil genesis analogues from South Westland (~43°S) and Taranaki-Wanganui (~39°S) regions in New Zealand, to provide new insights to better characterise and define the glacial chronostratigraphy in southern continental Chile.

2. Soil and loess stratigraphy

Soil formation is most often presented as occurring in a top-down sense, i.e., a set of processes acting on a pre-existing body of sedimentary or volcanic deposits or rock (the parent material) such that the degree and depth of alteration increases with time with a downward moving 'front' (Simonson, 1959). Such a scenario is clearly a simplification that nevertheless can hold true for many situations, but in aggrading landscapes where material is intermittently added to the ground surface this conceptual scheme is generally unsuitable (Nikiforoff, 1949; Raeside, 1964). Soils on surfaces incrementally mantled by loess, tephra, overbank deposits, colluvium or other materials form contemporaneously with the geological additions (of sediment, tephra, etc.), i.e. these soils formed by upbuilding (Nikiforoff, 1949). The degree of soil expression is dependent on the relative rates of geological accumulation and pedogenic alteration. Where the former dominates, the latter deposits are minimally modified and the geological material thickens without significant soil alteration. This scenario has been referred to as retardant upbuilding (Johnson and Watson-Stegner, 1987). Where rates of geological accumulation are low but where environmental factors drive high rates of pedogenesis (such as in warm and moist climates) coeval geological

accumulation and soil modification result in thick, strongly expressed soils (developmental upbuilding: Johnson et al., 1990; Lowe and Tonkin, 2010; Lowe et al., 2015). An important feature of upbuilding pedogenesis is that all depth increments of an up-building soil have experienced processes characteristic of surface horizons, such as melanisation, acidification, intense bioturbation and eluviation. As a surface soil horizon (typically an A horizon) becomes progressively buried by ongoing sediment or tephra accumulation it moves into a zone characterized by subsurface pedogenic processes (e.g. illuviation) and different moisture, temperature and bioturbation regimes. Moreover, features inherited from the near-surface pedogenic processes may modulate subsurface pedogenesis (McDonald and Busacca, 1990). Phases of up-building and topdown pedogenesis alternated during climatically modulated loess accumulation in the Quaternary. In relatively dry continental regions with extensive loess sources, loess accumulation in cold periods resulted in retardant upbuilding, which was followed by topdown pedogenesis in the warm periods when loess accumulation effectively ceased. These circumstances yielded the so-called loess-paleosol sequences of Europe, China, North America and the drier eastern side of the Andes (i.e. Chaco–Pampean plains and the northwest mountain environments of Argentina, Paraguay, Brazil, Uruguay, Bolivia; see Zárate, 2003 and references therein). In maritime New Zealand, particularly on the western side of the two main islands, high rainfall results in rapid pedogenesis, and, where loess accumulation rates have been relatively low (Eden and Hammond, 2003), loess accumulation phases resulted in developmental pedogenesis. In these circumstances there is no clear distinction between loess and paleosols; all the loess is altered by pedogenesis to a greater or lesser extent and at times there is pedogenic overprinting between loess sheets (Lowe et al., 2015). On the western side of North Island multiple incremental contributions of weatherable andesitic tephra have enhanced pedogenesis. During cold phases, developmental upbuilding occurred during accumulation of mixed andesitic tephra-aeolian deposits (Sy beds of Alloway et al. (1992a), now manifested as weak-to-moderately-structured, yellowish-brown moderately allophanic Bw horizons). Occurring within intervening warm phases, developmental tephra upbuilding continued but the intensity of pedogenesis increased. This scenario resulted in the accumulation of strongly weathered andesitic tephra soil material now manifested as well-structured, reddish-brown highly allophanic Bw horizons (Sr beds of Alloway et al. (1992a)).

On the West Coast of New Zealand's South Island, very high rainfall rates (>3-m annually) promote rapid pedogenesis (Tonkin and Basher, 2001) and consequently the relatively thin loess sheets characteristic of the region are strongly pedogenically altered from the overprint of developmental upbuilding and top-down pedogenesis. In well-drained environments, buried soils are identified by the occurrence of repeating E-Bs horizon pairs (Almond et al., 2001) (Fig. 1). At these sites, mineralisation of organic matter from the A horizon as it becomes buried reveals a bleached horizon subsequently identified as a buried E horizon (e.g., bE in the New Zealand Soil Classification, (NZSC: Hewitt, 2010), or Eb horizon in 'Soil Taxonomy' (Soil Survey Staff, 2014); see Fig. 1 caption for further explanation). Further addition of loess
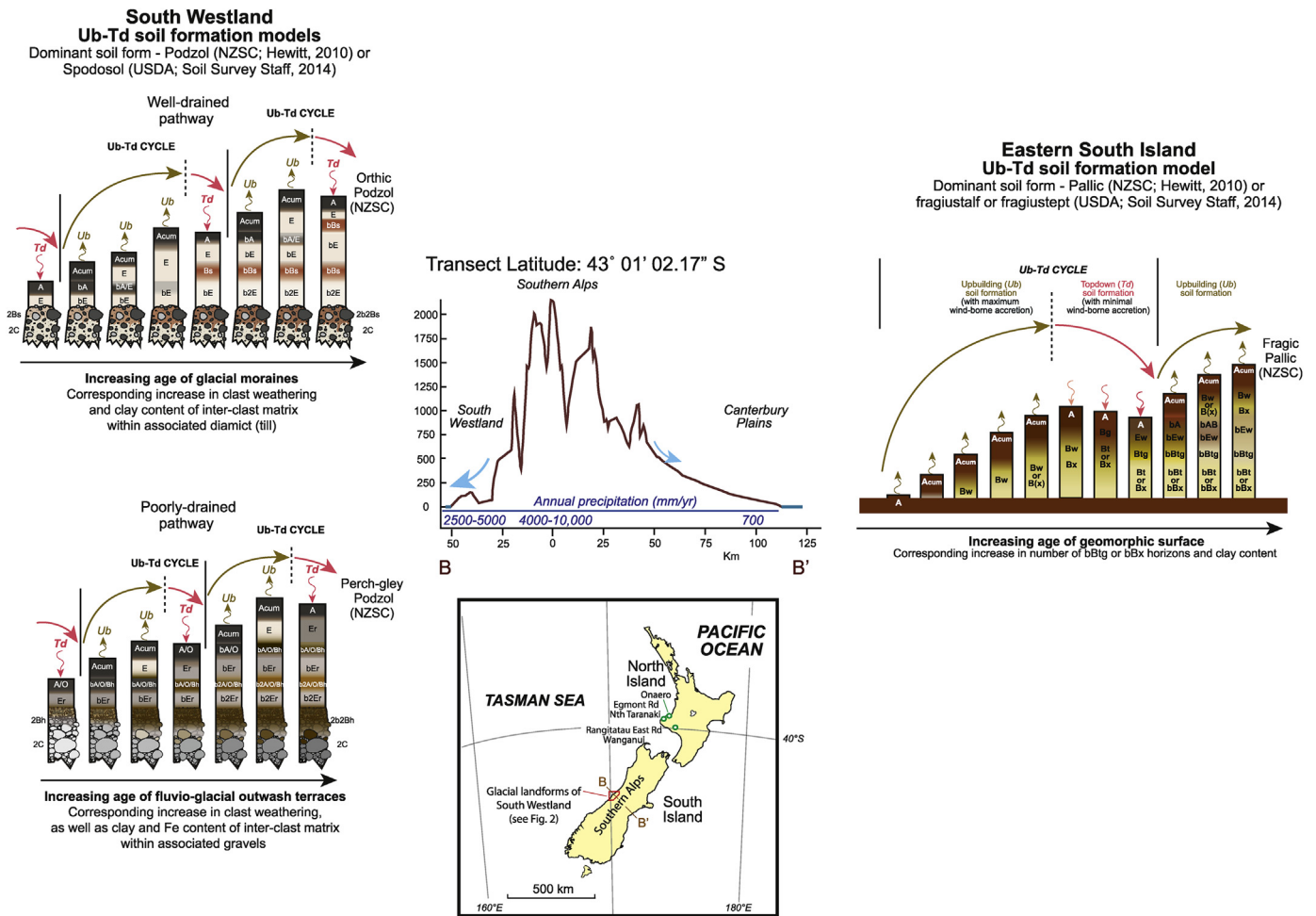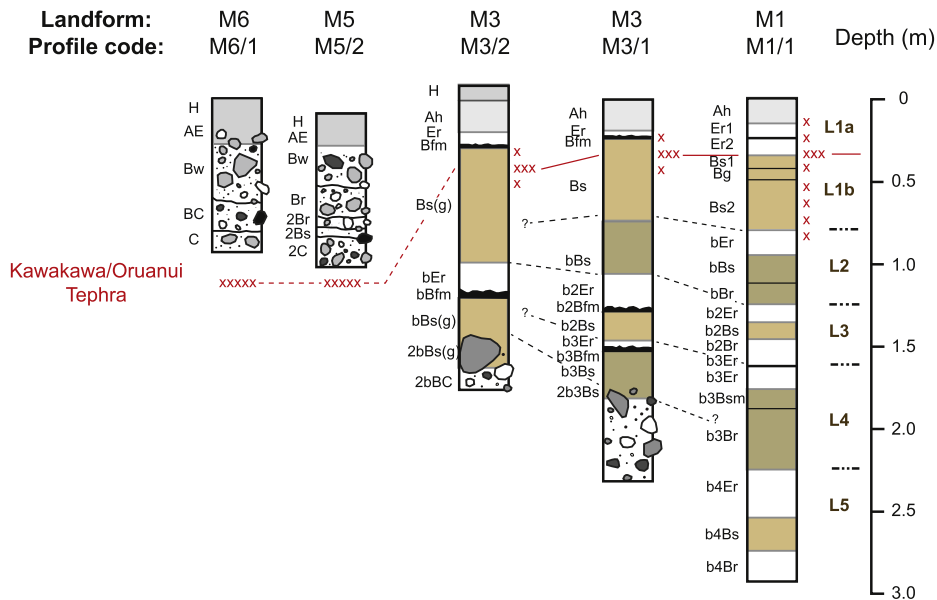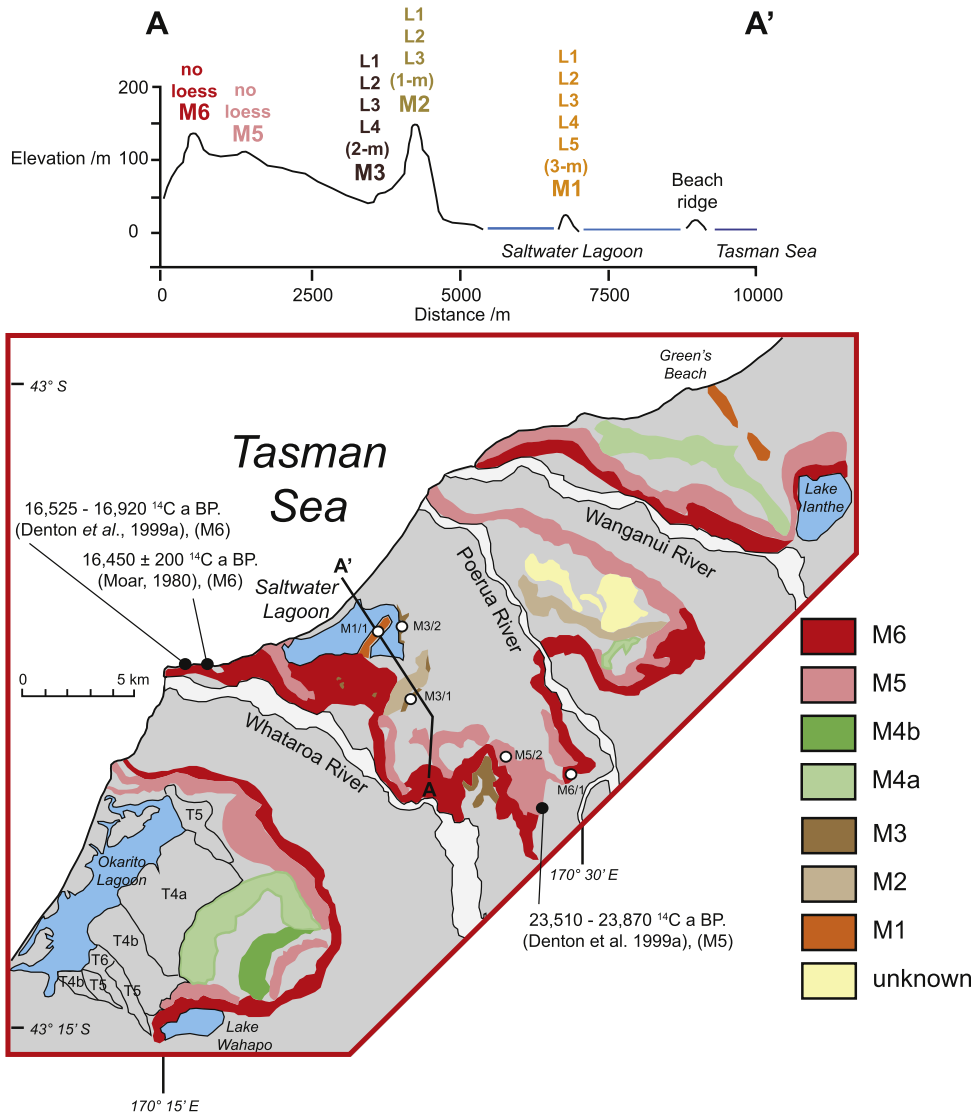
Fig. 1. Conceptual models of upbuilding (*Ub*) and topdown (*Td*) soil formation for multisequal soils formed from loess in a transect (~41°37′S) extending across South Island, New Zealand. In South Westland, which receives between 2500 and 5000-mm of average annual precipitation, *Ub-Td* soil formation on well-drained sites (glacial drift) typically form Orthods (Soil Survey Staff, 2014), equivalent to Orthic Podzol Soils (Hewitt, 2010) (top left panel), whereas poorly-drained sites (glacio-fluvial outwash) form Aquods or Perch-gley Podzol Soils (lower left panel; Hewitt, 2010; Almond and Tonkin, 1999; Almond et al., 2001; Soil Survey Staff, 2014). In eastern South Island, with <700-mm of average annual precipitation, *Ub-Td* soil formation typically form Fragiustalfs or Fragiustepts or Pallic Soils (top right panel; Hewitt, 2010; Lowe and Tonkin, 2010; Soil Survey Staff, 2014). The location of key sections described in Taranaki-Wanganui regions of western North Island (see Fig. 6) are indicated in the inset map of New Zealand. Note that the horizon notation represented in this figure (as well as for Figs. 2 and 5) is based on 'Horizon Notation for New Zealand Soils' (Clayden and Hewitt, 1994). The prefix 'b' denotes an identifiable soil horizon with pedogenic features developed before its burial. The following Arabic numeral indicates the numerical sequence of buried soils from the surface, although the numeral 1 is omitted in the case of the first buried soil. This scheme differs from 'Soil Taxonomy' (Soil Survey Staff, 2014) where 'b' for buried is a suffix rather than prefix.

results in weathering and translocation of Fe and Al from the upbuilding A and E horizon to lower increments. The result is an upbuilding Bs horizon (Almond and Tonkin, 1999). On less well-drained fluvio-glacial outwash terraces, buried soils are identified by the occurrence of repeating buried A/O/Bh-Er horizon pairs. In the anaerobic subsoils, organic matter in the A/O horizons does not mineralise as it becomes buried and secondary Fe minerals do not accumulate because of the reducing conditions. Aluminium extracted by acid ammonium oxalate solution (Al_{ox}) is generally accepted to be associated with nanocrystalline or short-range order minerals (e.g. McKeague, and Day, 1966) and is mobilised at low pH. In the presence of organic ligands, Al_{ox} precipitates at depth, particularly where it can further complex with buried organic matter. When loess addition stops or becomes negligible, topdown modification of the upbuilding soil continues with intensified translocation of Al whereby the maximum concentration of extractable secondary Al develops in the buried A and/or O horizons.

In drier eastern parts of both main islands of New Zealand

where loess accumulation rates tend to be higher (Eden and Hammond, 2003) and away from significant tephra inputs, loess sequences take on a character more similar to the more classically described loess-paleosol sequences described for the northern hemisphere as well as for the drier, eastern side of the Andes. The boundaries between loess sheets are defined by the tops of buried soils with an fragiustalf or fragiustept form in 'Soil Taxonomy' (Soil Survey Staff, 2014) (Pallic Soil in the New Zealand Soil Classification, NZSC: Hewitt, 2010), namely a dense, often prismatic-structured, fragipan (Bx horizon) usually overlain by a horizon with conspicuous redoximorphic features (Bg horizon) (as defined in Soil Survey Staff, 2014) (Fig. 1). Often loess sheets are in the order of metres-thick (Tonkin et al., 1974) and within a loess sheet there is a clear distinction between basal loess of minimal pedogenic alteration and the overlying soil formed in the upper part of the loess sheet. This stratigraphy represents retardant upbuilding during loess accumulation followed by developmental upbuilding in the intervening warm phases. Nonetheless, there is evidence to indicate that the fragipan is at least partly a consequence of pedogenesis during

Elevation /m — A to A' topographic profile and geological map of the Tasman Sea / Whataroa River region showing landform units M1–M6 and loess sequences L1–L5, with profile columns for M6/1, M5/2, M3/2, M3/1 and M1/1 depth profiles.

the loess accumulation phase (Kemp et al., 1998), and that topdown pedogenesis results in a range of features including formation of redoximorphic horizons, clay illuvial (Bt) horizons, gley veins between prisms in the fragipan and general degradation of the fragipan (Bruce, 1973, 1996).

The inferred climate control on loess accumulation (upbuilding pedogenesis: developmental or retardant), and cessation of the loess flux (topdown pedogenesis) is supported by paleobotanical studies and chronology. Direct dating of loess has typically been confounded by contamination by young carbon of samples submitted for radiocarbon-analysis (Goh et al., 1978), and problems associated with the systematics of luminescence dating (Berger et al. 2001a,b; 2002). However, tephrochronology (Palmer, 1982c; Alloway et al., 1988, 1992a; 2007; Pillans, 1988; Pillans et al., 1993; Eden, 1989; Berryman, 1992; Almond, 1996; Litchfield and Reiser, 2005; Litchfield and Berryman, 2005; Hughes et al., 2009, 2010; Vandergoes et al., 2013) has provided constraining ages for loess sheets and confirmed their deposition during cold climate phases. Pollen and phytolith-based reconstructions of past vegetation show loess accumulation occurred during times of widespread grassland and shrubland vegetation (Raeside, 1964; Kondo et al., 1994; Carter and Lian, 2000; Almond et al., 2001) whereas topdown pedogenesis occurred during periods when taller-statured vegetation, including forest, dominated. Independent well-dated pollen records (Alloway et al., 2007 and references therein) have unequivocally shown these vegetation transitions to be climatically controlled such that they have become the basis for defining New Zealand's climate event stratigraphy (Barrell et al., 2013).

3. Glacial records

3.1. South Westland, New Zealand

In South Westland, six distinct moraines and associated outwash terraces were recognised (Almond, 1996, Almond et al., 2001, Fig. 2), each of which was interpreted to represent a separate glacial advance. Moraines are designated M6, M5, etc. in order of increasing age and their associated outwash terraces are correspondingly designated T6, T5, etc. Relative ages were assigned to moraines using the principle that moraines become progressively younger toward the Southern Alps because early moraines within the range of a later glacial advance are obliterated. The three oldest moraines (M1, M2, and M3) lie within Saltwater Forest and are sub-parallel to the coastline. The age of the youngest moraines (i.e. M6 and M5) were supported by an array of radiocarbon dates (Moar, 1980; Denton et al., 1999b) and also by the occurrence of the ~25.4 cal ka BP Kawakawa/Oruanui Tephra (KOT; Almond, 1996; Almond et al., 2001; Vandergoes et al., 2013) which has recently been identified distally within the WAIS Divide ice core, West Antarctica (Dunbar et al., 2017). Loess cover-beds thickened and the number of buried soils increased systematically with the age of the landforms they mantled. A maximum of five loess sheets and morphologically identified soil features were recognised.

Accumulation of South Westland loess sheets has been linked via chronology and palynology to cool/cold climate conditions (Almond, 1996; Almond et al., 2001). Synchronicity of fluvial aggradation and loess accumulation points to the linking

mechanism or mechanisms, namely broad, aggrading and unstable outwash plains formed during glacial advances create extensive loess sources. Nonetheless, loess continues to accumulate in the Holocene, albeit slower and more spatially limited (Eger et al., 2011, 2013; Marx and McGowan, 2005), despite rivers being confined to relatively narrow, well-vegetated floodplains. The braided rivers issuing from the Southern Alps range front drain catchments with specific sediment yields exceeding $5000 \, t \, km^{-2} y^{-1}$ (Hicks et al., 2011) and their braided and flood-prone channels still provide a significant loess source. At the only site of detailed study, Haast River, Holocene loess forms a narrow loess wedge (c. 1 km-wide) downwind of the predominant westerly-quarter winds (Eger et al., 2012). The rapid downwind thinning implicates the tall rainforest in 'scrubbing' of loess from the atmosphere. Contemporary aeolian processes provide insights into the faster and more widespread loess accumulation during stadials. At these times the broad outwash plains forming in front of the glacial termini constituted a larger source area, while other factors such as lower rainfall, shorter-stature vegetation, and stronger winds may have contributed as well.

3.2. Southern continental Chile

Dominant features of the southern continental Chile landscape are ubiquitous moraines, outwash plains and ice-carved lake basins formed by Andean piedmont glaciers during episodes of cold (glacial) episodes through the Quaternary. The extent and relative-ages of glaciated landform-sediment sequences extending over the last glacial period in northwest Patagonia are well known (e.g. Andersen et al., 1999; Denton et al., 1999b). At least three ridge-forming glacial drift deposits have been recognised extending westwards from the Andean range front (Fig. 3). The two oldest deposits (locally referred to as Casma and Colegual Drift, Mercer, 1976) represent pre-last glacial drift and associated outwash plains, which become progressively more subdued in their topographic expression and have a steadily increasing thickness of layered fine-textured loess-like cover-beds (now weakly developed soil horizons) formed from wind-borne accretion, towards the west.

Glacial coverage during MIS 4 is based on minimum ^{14}C ages of ~40–50 cal ka and pollen analyses from cores retrieved within Taiquemó mire (Heusser et al., 1999; Heusser and Heusser, 2006). The youngest glacial drift deposits (locally referred to as Llanquihue Drift) represent the last glaciation, and are mostly coincident with the maximum western-most extent of lakes within the Chilean Lake District. Radiocarbon dating of Llanquihue landforms show that the Andean ice lobes advanced into the moraine belt depicted in brown in Fig. 3 numerous times during cold-cool inter-stadial phases of Marine Isotope Stage (MIS) 3 and 2 (Denton et al., 1999b; Heusser et al., 1999). Lisiecki and Raymo (2005) date stage boundaries from benthic $\delta^{18}O$ records (LR04 stack) to 57 ka (MIS 4–3), ~33 cal ka BP (MIS 3–2), and ~17 cal ka BP (MIS 2–1). The chronology of glacial advance in southern continental Chile during the LGM (~33,400 to ~17,800 cal a BP) is constrained by an extensive array of ^{14}C dates from sites tied to the former Llanquihue, Reloncaví, Ancud and Golfo de Corcovado ice lobes (Denton et al., 1999a,b; Moreno et al., 2015). LGM glacial advances in this region

Fig. 2. A. Glacial landforms of South Westland (modified from Almond, 1996; Almond et al., 2001). The location of this area is indicated on the inset map of New Zealand (see Fig. 1). Moraines are designated M6, M5, etc. in order of increasing age and their associated outwash terraces are correspondingly designated T6, T5, etc. The three oldest moraines (M1, M2, and M3) lie within Saltwater Forest and are sub-parallel to the coastline. The locations of key radiocarbon sample sites in this area are indicated (Moar, 1980; Denton et al., 1999a). B. Soils and loess stratigraphy of moraines (M6 to M1; youngest to oldest) occurring within Saltwater Forest. Note the persistent occurrence of the New Zealand-wide LGM-aged chronomarker Kawakawa/Oruanui (KOT) Tephra (dated at c. 25,358 ± 162 cal a BP; Vandergoes et al., 2013) occurring in the upper part of the profiles of pre-LGM moraines (M3, M1) and at the contact between L1a and L1b. An elevational transect (A-A′) across these moraines extending from the foothills of the Southern Alps to the coastline are indicated as well as the number of loess horizons mantling each moraine.
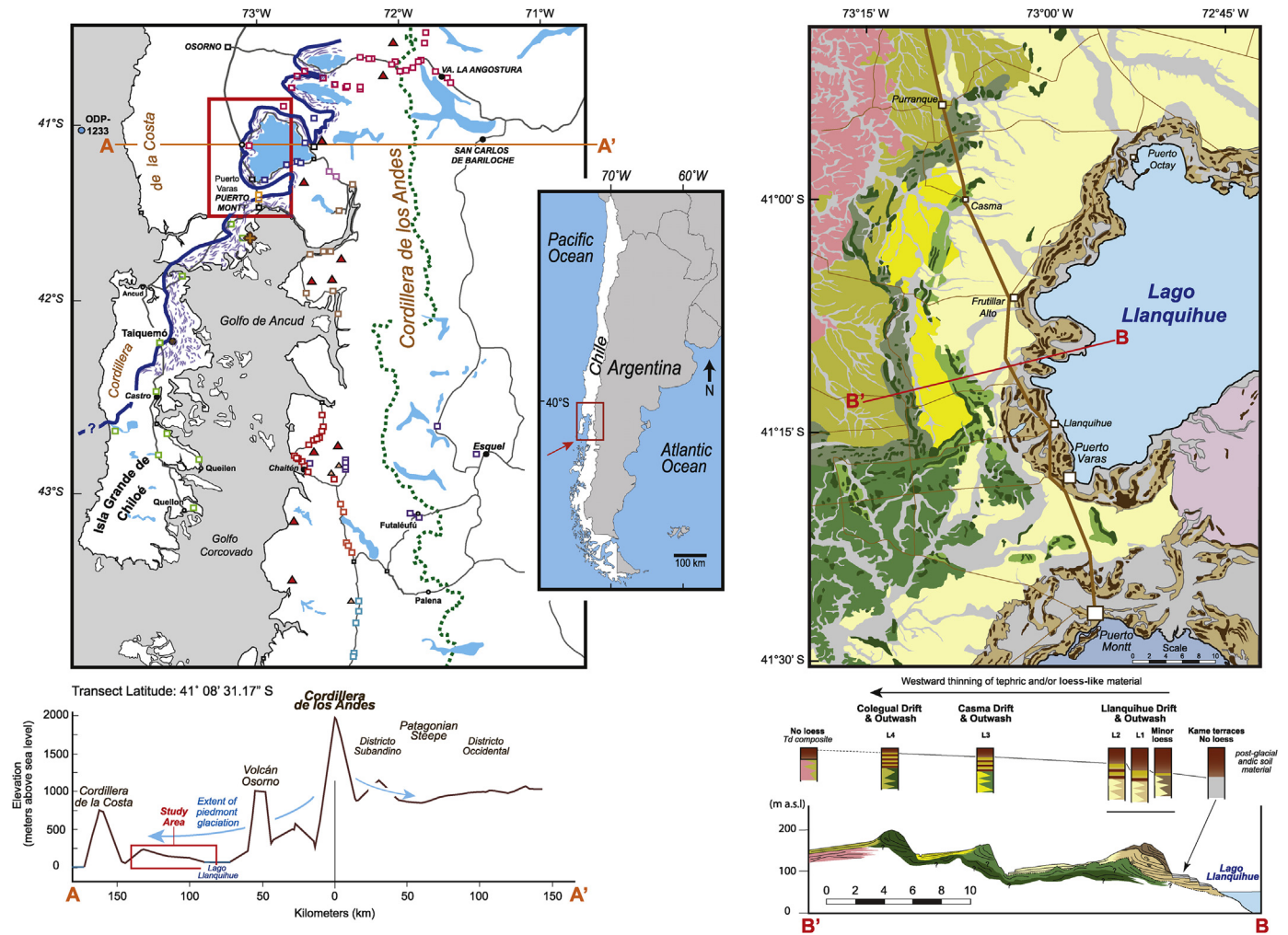
Fig. 3. A. The location of the study area in Llanquihue-Puerto Montt, Hornopirén, Chaitén and Isla Grande de Chiloé sectors of northwestern Patagonia. The extent of ice lobes within this region during the Last Glacial Maximum (LGM) (modified from Plates 1–4 in Denton et al., 1999b) is indicated by a solid blue line extending north to southwest. Moraine ridges or hills associated with these ice lobes are indicated in purple. The location of the Huelmo mire (Moreno and Leon, 2003; Moreno et al., 2015) is indicated as a star symbol. In this immediate vicinity, seven boulders were sampled from adjacent moraines for ¹⁰Be surface-dating (see also Fig. 4). An elevational transect (*A-A'*) across northwest Patagonia (~41°08′S) is also indicated. B. Glacial geomorphic map of the Llanquihue-Puerto Montt area (modified from Andersen et al., 1999) showing Llanquihue (brown), Casma (green) and Colegual (dark green) moraine belts and associated outwash plains. Meltwater spillways, lake-bordering kame terraces, and areas dominated by volcaniclastic deposits sourced from an ancestral Volcan Calbuco are also indicated. A schematic cross-section (*B-B'*) of this drift-outwash succession is indicated and shows a multisequal arrangement of soil-cover-beds predicted to occur on successively older glacial-outwash deposits. Note the westward thinning of tephric and/or loess-like andic soil material and increased occurrence of pedogenically overprinted older subsurface soil horizons forming composite upper profiles. (For interpretation of the references to colour in this figure legend, the reader is referred to the Web version of this article.)

have been recorded at ~33,600, ~30,800, ~26,900, ~26,000 and 18,100-17,700 cal a BP. There appears to be significant differences in the extent of these lobes during the glacial advance at ~18 cal ka BP as evidenced by the two northern lobes (Llanquihue and Reloncaví) reaching the inner margin of the LGM moraine belt whereas the two southern lobes (Ancud and Golfo de Corcovado) was either the most extensive, or close to the most extensive during MIS 2.

4. Cosmogenic dating in the Chilean Lake District

In Patagonia, besides sporadic ⁴⁰Ar/³⁹Ar dated lava-flows (e.g., Singer et al., 2004), or possibly OSL on associated sediments (Smedley et al., 2016), cosmogenic nuclide dating is currently the only other approach available for dating landforms older than Stage 3. However, there are two potential problems that affect the application of cosmogenic dating to older landforms. First, this technique appears to so far provide only minimum-limiting ages on

moraines older than the last glacial cycle (e.g., Stage 6 and older) due to the effect of geomorphic processes such as boulder exhumation. Dating outwash plain remnants is more robust and has allowed direct age constraints on outwash dating to Stage 8 and as old as 1 Ma (Hein et al., 2009, 2017). However, for each glacial outwash facies, the method is time consuming and relatively expensive given the amount of analyses needed (e.g., Hein et al., 2010). Second and in the context of this study, dating even LGM-aged landforms in the wettest areas of the Chilean Lake District appears not to be possible, as we show here. To test the viability of cosmogenic dating in this region, given a former dense rainforest now mostly cleared for agriculture, we measured ¹⁰Be concentrations in 7 samples near the Huelmo mire (Moreno and Leon, 2003; Massaferro et al., 2014, Fig. 4). The timing of deglaciation at Huelmo and surrounding area is well-dated (Andersen et al., 1999; Denton et al., 1999a,b; Moreno et al., 2015). Specifically, at Huelmo, ice recession over the site is tightly constrained to ~19.5−19.6 cal ka.
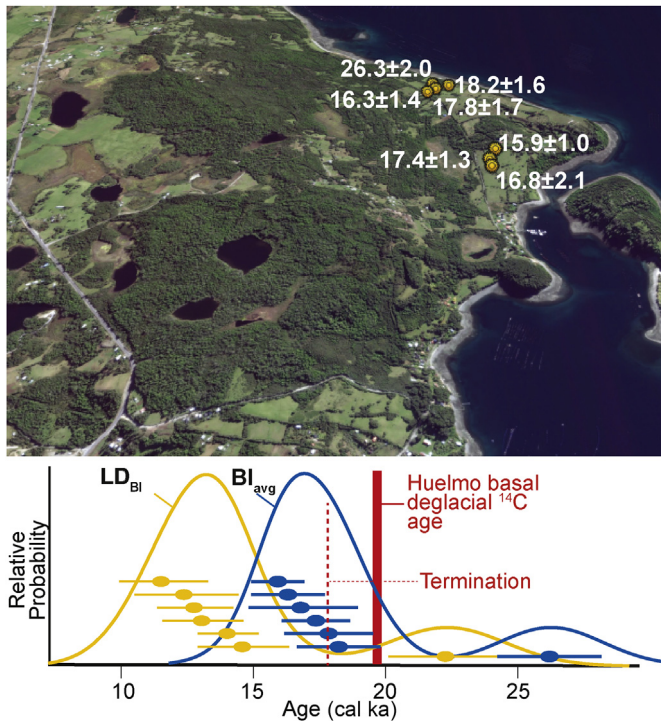
Fig. 4. Sample location and [10]Be data for 7 samples near the Huelmo mire (Fig. 3; see also Table 1), shown as individual ages (±1σ) and summed probability density (thick line) plots. In Table 1 and the bottom panel, we present two sets of ages because the procedural blank (Bl) run with the seven samples was above average for the laboratory (BL$_{avg}$). Regardless of the blank used, all ages are younger than the Huelmo mire basal (deglacial) ^{14}C ages (indicated by the red solid line at ~19.5–19.6 cal ka; see Moreno and Leon, 2003; Moreno et al., 2015). The top panel shows (older calculated) ages with average blank, overlain on a Google Earth image. (For interpretation of the references to colour in this figure legend, the reader is referred to the Web version of this article.)

Moreover, as summarized below, the Termination in the region occurred ~17.8 cal ka (Fig. 4); this includes in the inner Andes, well east of Huelmo and Chiloé.

Samples were processed using standard procedures at the University of Edinburgh, measured at the Paul Scherrer Institut in Zurich, and then calculated with the regional Patagonian rate and systematics discussed in Kaplan et al., (2011) (e.g., v.2.2 of the CRONUS calculator). We present two different sets of ages because the procedural blank run with the seven samples was above average for the laboratory (Table 1). Hence, we also show ages with the average blank value over several years (summarized in Kaplan et al., 2007). A key point is, regardless of the blank used, except for one anonymously old age (sample LD-02-03), all ages are younger than the Huelmo deglacial ^{14}C ages (see Fig. 4), and are generally younger than the Termination age east (up-flow) of the Lake District (Moreno et al., 2015). With the higher background level, the ages are, on average, thousands of years too young. All [10]Be ages presented are based on the Lm scaling (Lal, 1991; Stone, 2000; Balco et al., 2008) of the high latitude, sea-level Patagonian production rate (Kaplan et al., 2011) to the specific location and elevation of the sample.

We offer two possibilities to explain why [10]Be ages from this sector are too young. The first may relate to shielding by rainforest vegetation and its forest-floor. For stand-alone (erratic) boulders and/or those protruding from the ground surface, direct field observations indicate vegetative growth extending up from the forest floor to ultimately wrap around and cover the top of these boulders. Moreover, the rainforest floor provides a surface where continued

upbuilding of sediment and ash-fall material can occur. Second, since deglaciation, many areas of the Chilean Lake District have been frequently inundated by volcaniclastic mass-flows sourced from adjacent Andean eruptive centres (Andersen et al., 1999; Denton et al., 1999b; Moreno et al., 2015). In road-cuts and gravel pits, these volcaniclastic mass-flow deposits can be often observed to encapsulate and bury glacially emplaced boulders and, in some cases, glacial boulders have also been directly incorporated within the mass-flow itself during its passage across the landscape. Anomalously young [10]Be ages acquired from an already well-dated site in a formerly densely vegetated hyper-humid environment highlight the difficulties associated with this technique, specifically in such settings (as noted above). This outcome clearly affirmed why a soil cover-bed approach has been a useful additional tool for inferring the age of glacial advances in this region of Patagonia.

5. Presence of multisequal andic soil successions

An important aspect that connects southern continental Chile with New Zealand is the widespread occurrence of andic-dominated cover-beds. In both the Soil Taxonomy (Soil Survey Staff, 2014) and New Zealand Soil Classification (NZSC; Hewitt, 2010) Andisols or Allophanic Soils (respectively) are predominantly formed from well-drained tephra or volcanic ash and, defined as containing high proportions of glass and nanocrystalline colloidal materials, including allophane and ferrihydrite along with paracrystalline imogolite (e.g. Churchman and Lowe, 2012). In New Zealand, Andisols (or Allophanic and Pumice Soils in NZSC) cover 12.5% of the country and are predominantly associated with the tephra products of rhyolitic to andesitic volcanic centres of central and western North Island (Lowe and Palmer, 2005), but allophanic Inceptisols (Allophanic Brown Soils in NZSC) can also form from the weathering products of greywacke and schist in the South Island high country (Hewitt, 2010). Typically, these soils have distinct 'andic' properties of high 1500 kPa (15-bar) water retention, high porosity and low bulk density, and are dominated by nanocrystalline materials chiefly allophane, ferrihydrite and metal-humus complexes (Parfitt and Clayden, 1991; McDaniel et al., 2012; Soil Survey Staff, 2014).

In southern Chile (36-49° S), Typical (*trumaos*) and Aquic (*ñadis*) Andisols are well expressed in areas west of, and adjacent to, volcanic centres of the Cordillera de los Andes and extend down the longitudinal Central Valley south of 36° S (FAO-UNESCO, 1971; Luzio et al., 2010; Casanova et al., 2013). Their occurrence is coincident with Holocene-aged Andean-sourced tephra deposits on fluvial and fluvio-glacial landforms. Trumaos are characterised as deep, well-drained soils (Hapludands) occurring on moderate to steep slopes whereas ñadis are moderately deep, poorly drained soils (Placaquands) occurring on flat or depressed positions in the landscape (Casanova et al., 2013). In both southern Chile and western to central regions of New Zealand's North Island, cover-bed sections proximal to volcanic centres typically comprise predominantly tephra-derived, fine-textured soil materials separating thick and/or coarse-grained lithologically distinct tephra beds and volcaniclastic detritus that have resisted post-depositional weathering and pedogenic mixing. At medial to distal locations from volcanic sources, however, the proportion of fine-textured soil material significantly increases as tephra becomes perceptibly thinner and finer-textured. Each andic inter-bed forms part of a soil accession and represents a period of intermittent accretion of fine-grained detritus (dominantly tephra) with concomitant rapid weathering (Alloway et al., 1995) (see Section 2 above *Soil and loess stratigraphy*).

In southern continental Chile, the post-glacial andic soil succession developed on glacial, glacio-fluvial and volcanic landforms

Table 1
Surface-exposure sample details and 10Be ages.

Sample	Latitude (DD)	Longitude (DD)	Elevation (masl)	Quartz weight (g)	Carrier (Be) added (g)	$^{10}Be/^9Be \pm 1s$	$[^{10}Be] \pm 1s$ (atoms g^{-1})	^{10}Be Age $\pm 1s$[a] (yrs)	^{10}Be Age $\pm 1s$[b] (yrs)
LD-02-01	−41.643	−73.0662	50	31.2658	0.255198	0.1439 ± 0.01250483	67384 ± 5856	16300 ± 1400	13100 ± 1600
LD-02-02	−41.6423	−73.0647	60	15.8872	0.207602	0.1105 ± 0.01053817	74581 ± 4466	17800 ± 1700	11500 ± 1700
LD-02-03	−41.6421	−73.0659	58	25.1526	0.255099	0.1837 ± 0.01372043	110723 ± 6304	26300 ± 2000	22300 ± 2200
LD-02-04	−41.6427	−73.0657	57	27.8114	0.256682	0.1435 ± 0.01235303	76020 ± 4561	18200 ± 1600	14600 ± 1800
LD-02-05	−41.6489	−73.0624	26	23.4161	0.256781	0.1131 ± 0.01383996	68032 ± 5495	16800 ± 2100	12400 ± 2000
LD-02-06	−41.6478	−73.0621	43	54.7563	0.253615	0.2313 ± 0.01493313	65275 ± 3405	15900 ± 1000	14100 ± 1200
LD-02-07	−41.6484	−73.0625	31	22.3352	0.202555	0.1421 ± 0.01069512	70549 ± 3652	17400 ± 1300	12800 ± 1400
Average lab blank					0.257177	0.0203 ± 0.006063			
LD_BLK					0.257177	0.0450 ± 0.01332			

[a] Average laboratory blank (Bl).
[b] Individual blank (LD).

and/or surfaces, is of dominantly volcanigenic-provenance as evidenced by the thickening towards multiple volcanic sources centred eastwards and along the Cordillera de los Andes. This situation contrasts with South Westland, New Zealand, where layered soil successions mantling glacial and glacio-fluvial landforms have completely different soil attributes on account of the quartzo-feldspathic provenance of the cover-beds (no tephras nor volcanics), significantly higher precipitation (>3-m per annum) and extreme organic translocation and acid leaching conditions. Consequently, soils in this region are dominantly categorised as Spodosols (Soil Survey Staff, 2014) or Podzol Soils (NZSC; Hewitt, 2010). Layered andic soils of Wanganui-Taranaki in western North Island (see Fig. 2 inset) have soil attributes more akin to those andic soils occurring in southern Continental Chile and are similarly of dominantly volcanigenic origin. Instead of andic soils mantling glacial landforms as is the case for southern continental Chile, andic soils of western North Island typically form on uplifted alluvial and marine terraces as well as on volcaniclastic deposits adjacent to source volcanoes.

On the western side of the Andes soil genesis appears to be dominated by a flux of intermittently erupted Andean-sourced tephra which has continued to upbuild soils at the ground surface separated by intervals where topdown weathering processes are intensified. Alternating layers of reddish-brown (Sr-) and yellowish-brown (Sy-) soil horizons can be occasionally observed upon old drift deposits (Casma-Colegual). Sr-horizons have reddish-brown to brown hues (5YR-7.5YR) with high chroma and are characteristically well-developed with a fine to medium blocky-structure, whereas the Sy-horizons are moderately to poorly developed coarse blocky structured to massive with yellow-brown hues (10YR-2.5YR) and high chroma. Sr-horizons are laterally continuous and typically uniformly thick whereas Sy-horizons are laterally discontinuous and may have erosional basal boundaries that cross-cut older andic soil horizons. A conceptual model of upbuilding (Ub) and topdown (Td) soil formation for this region is presented in Fig. 5. With increasing number of reddish-brown (Sr-) and yellowish brown (Sy-) soil horizon (Bw) couplets there is a corresponding increase in coupled Ub-Td cycles. As already demonstrated by New Zealand studies (i.e. Fig. 6), multisequal soil successions have a clear implied connection to coupled glacial and interglacial climate cycles of the Quaternary.

In areas bordering Lago Llanquihue and coastal regions adjacent to Seno Reloncaví, Llanquihue glacial drift deposits have complex depositional architectures (Fig. 7A and B) with diamicts and ice-contact stratified sediments representing different-aged advances chaotically juxtaposed. Ice-contact sediments frequently exhibit syn-depositional deformation but in some cases, stratified sediments can be displaced by normal faults. Llanquihue drift and outwash gravels are identified by an eastward-thickening of fine-textured post-glacial andic soil material and coarsening tephra inter-beds (Fig. 7C and D). Occasionally, late Llanquihue drift can be observed to either directly overlie earlier Llanquihue drift deposits with a sharp and wavy erosional contact (Fig. 7E), or is sometimes observed separated by thin to moderate (<0.5-m) andic soil material resting on a gravel-lag pediment atop an older drift (Fig. 7F). In the vicinity of Casma, beyond the western limit of the LGM-ice lobe, laterally discontinuous yellowish-brown sandy-textured andic material sits directly upon Llanquihue outwash deposits (Fig. 7G), indicating localised accumulation of aeolian sands directly adjacent an outwash channel. In the same vicinity, multisequal soil horizons are observed intervening between successively older outwash deposits (Fig. 7H). Frequently associated with drift and outwash deposits of this region are sequences of non-cohesive volcaniclastic mass-flow deposits, likely sourced from an ancestral Calbuco Volcano, which bury and/or erode pre-existing surfaces (Fig. 8A–C). Exposed along Ruta 5, at a locality just north of Puerto Montt, a massive to weakly stratified debris-flow deposit containing pumice clasts and bread-crusted bombs surmounts and thins out over adjacent and more elevated LGM-age moraines (Fig. 8D and E).

On a newly exposed road section on Ruta 5 (km-1054.2) between Puerto Montt and Pargua (41°37′25.0′ S; 73°16′46.9′ W), a multisequal soil succession with four Sr-Sy couplets overlies a highly-weathered glacial diamict (till) with a ~4.2-m-long, large diameter (1-m+) tree-trunk mold encased within its matrix (Fig. 9A and B). At the northern end of this section, a sheet of Sy1 (of interpreted LGM-age) cross-cuts older soil horizons and thins southwards along section. At this southern point, Sy-1 is apparently overprinted above by Sr-1 top-down soil formation that penetrates into older pre-Sy1 soil horizons forming a composite profile.

A significant point of difference between multisequal soil records from New Zealand and Chile, is that andic soil sequences in New Zealand are frequently interbedded by widespread and distinct rhyolitic tephra layers sourced from the Taupo Volcanic Zone (TVZ), situated in the central North Island, which provide opportunities for independent chronological control (e.g. Fig. 6). In southern Chile, numerous late Last Glacial to Holocene-aged tephra deposits of variable composition can be recognised westward and upwind of the Cordillera de los Andes — the strong westerly winds favour dispersal to the east and few tephras are preserved any further west than the limits of the LGM and LGIT moraines (e.g. Watt et al., 2009; Fontijn et al., 2014; Alloway et al., 2015). So far, only two widespread tephra markers (Chana and Lepue Tephras, dated ~9.6 and ~11 cal ka BP, respectively) sourced from Chaitén
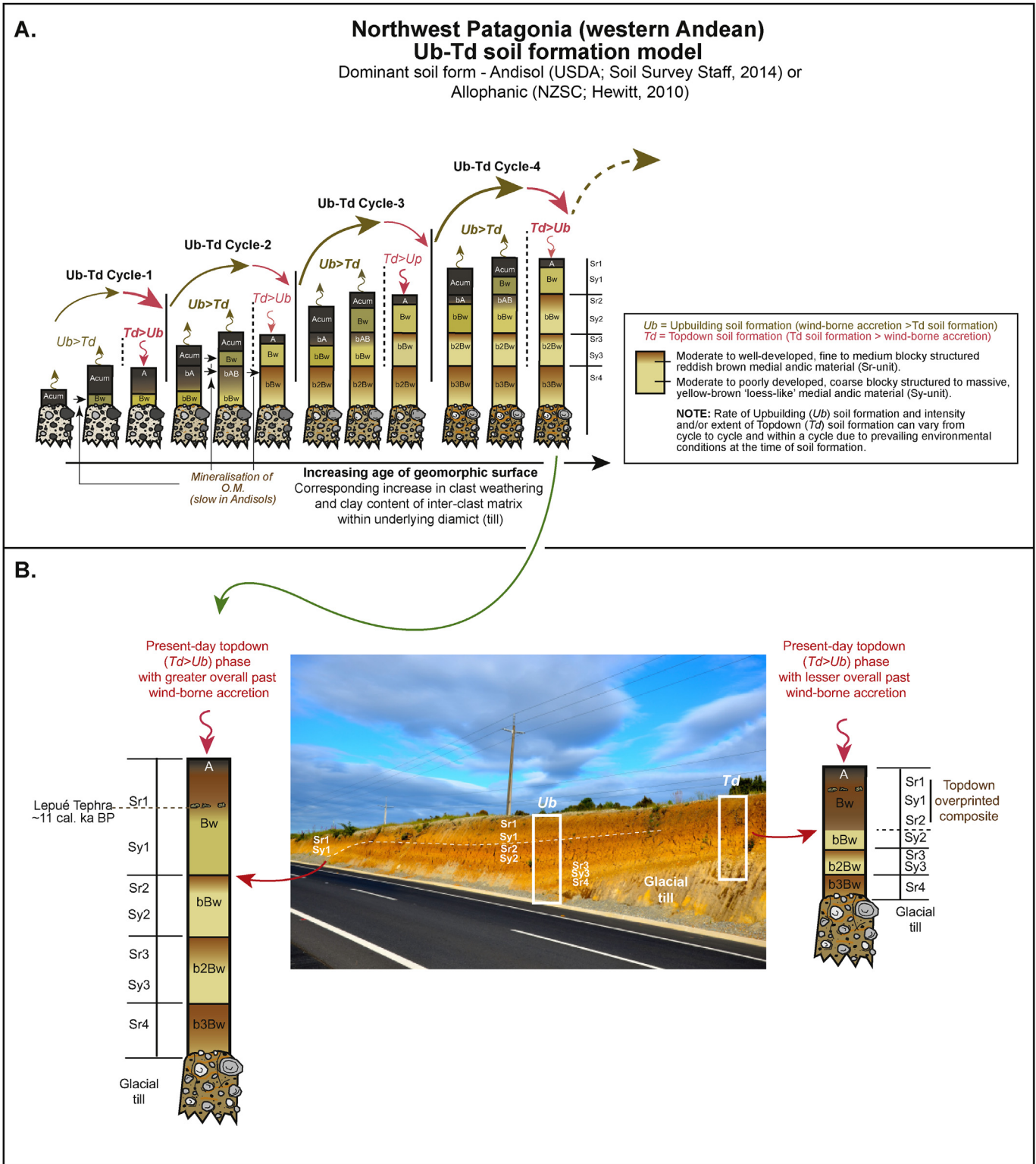
Fig. 5. A. Conceptual model of developmental upbuilding (*Ub*) and topdown (*Td*) soil formation in southern continental Chile. It is important to recognise that developmental upbuilding reflects the interplay of geological accumulation and concomitant (but only weakly effective) topdown pedogenesis. Topdown pedogenesis occurs with nil or negligible geological accumulation, and pedogenesis is thus much more effective and intense. With increasing number of coupled *Ub-Td* cycles there is a corresponding increase in reddish-brown (Sr-) and yellowish brown (Sy-) soil horizon couplets. Coupled *Ub-Td* cycles are associated with fluctuations in cool/cold-warm paleoclimate during the Quaternary, respectively. B. Road section on Ruta 5 (km-1054.2) between Puerto Montt and Pargua (41°37′25.0′S; 73°16′46.9′W) showing four Sr-Sy couplets overlying a highly-weathered glacial diamicton (till) with an encapsulated tree-trunk mold. In upslope portions of this section there appears to be lesser overall wind-borne accretion, as evidenced by significant post-glacial topdown soil formation that has pedogenically overprinted older subsurface soil horizons and formed a composite upper profile. (For interpretation of the references to colour in this figure legend, the reader is referred to the Web version of this article.)
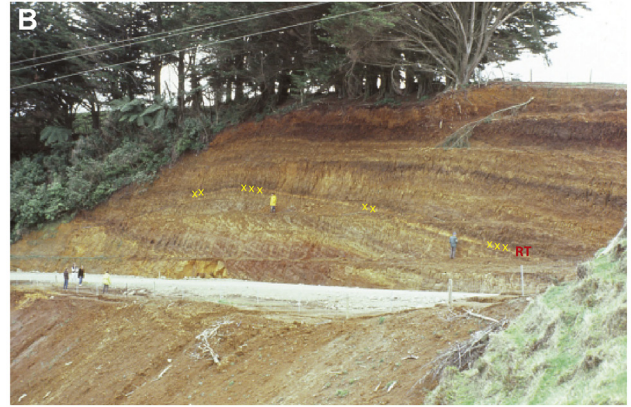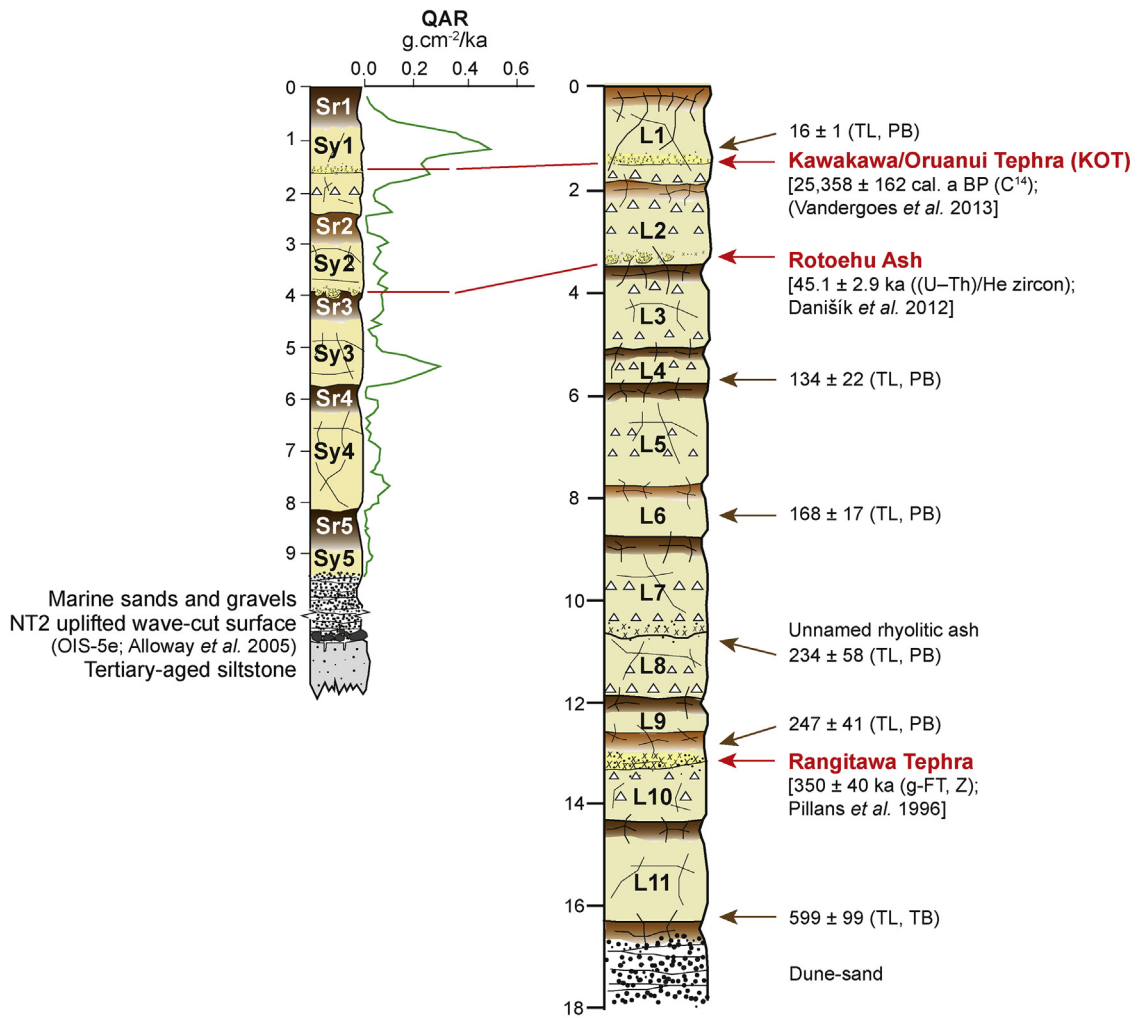
Western North Island
Dominant soil form - Allophanic (NZSC; Hewitt, 2010) or
Andisol (USDA; Soil Survey Staff, 2014)

Onaero,
North Taranaki
(Alloway *et al.* 1992a)

Rangitatau East Road,
Wanganui-Taranaki
(Palmer and Pillans, 1996)

QAR
g.cm^{-2}/ka

16 ± 1 (TL, PB)

Kawakawa/Oruanui Tephra (KOT)
[25,358 ± 162 cal. a BP (C^{14});
(Vandergoes *et al.* 2013]

Rotoehu Ash
[45.1 ± 2.9 ka ((U–Th)/He zircon);
Danišík *et al.* 2012]

134 ± 22 (TL, PB)

168 ± 17 (TL, PB)

Unnamed rhyolitic ash
234 ± 58 (TL, PB)

247 ± 41 (TL, PB)

Rangitawa Tephra
[350 ± 40 ka (g-FT, Z);
Pillans *et al.* 1996]

599 ± 99 (TL, TB)

Dune-sand

Marine sands and gravels
NT2 uplifted wave-cut surface
(OIS-5e; Alloway *et al.* 2005)
Tertiary-aged siltstone

Fig. 7. In areas bordering Lago Llanquihue and coastal regions adjacent to Seno Reloncaví, diamicts and ice-contact stratified sediments have complex depositional architectures (A, 41º45′44.4′S, 73º25′09.2′W; B, 41º13′33.8′S, 72º38′29.2′W). Llanquihue drift and outwash gravels are identified by an eastward thickening of fine-textured (medial-ashy grade) post-glacial andic soil material, as well as coarsening tephra inter-beds. C shows a typical post-glacial andic soil succession in the vicinity of Frutillar (41º07′26.6′S, 73º01′21.7′W), just inside the LGM glacial limit. No macroscopic tephra interbeds are evident. Further eastwards in the vicinity of Ensenada (41° 13′ 21.8′S, 72° 39′ 38.7W) and closer to eruptive centres situated in the Cordillera de los Andes, D shows Llanquihue drift overlain by multiple centimetre-thick, coarse-grained tephra and subordinate andic soil interbeds of post-glacial age. Occasionally, drift deposits are directly stacked on top of each other (E, 41º19′02.4′S, 73º00′28.7′W) separated by lag-gravel pediment, or are separated by prominent and laterally continuous well-developed andic soil material (F, 41º19′02.6′S, 73º00′34.1′′W). G. In the vicinity of Casma (41º01′59.0′S, 73º06′35.3′W) beyond the western limit of the LGM-ice lobe, laterally discontinuous yellowish-brown sandy-textured andic material (<0.6-m thick) sits directly upon Llanquihue outwash deposits indicating localised accumulation of aeolian material directly adjacent an outwash channel. H. In the same vicinity (41º00′25.9′S; 73º07′07.5′W), multisequal soils intervene between successively older outwash deposits. (For interpretation of the references to colour in this figure legend, the reader is referred to the Web version of this article.)

Fig. 6. Multisequal soil successions of dominantly volcanigenic (andic) provenance exposed at (A) Egmont Road, North Taranaki (39°03′ 09.06′S, 174°07′ 41.14′ E; Alloway et al., 1992a), and (B) Rangitatau East Road, Wanganui (Palmer and Pillans, 1996). These soil successions form the dominant cover-beds on uplifted marine terraces in western North Island, New Zealand. C. Stratigraphic profiles from Onaero, North Taranaki (Alloway et al., 1992a) and Rangitatau East Road, Wanganui (Palmer and Pillans, 1996), indicating multiple couplets of reddish-brown (Sr-) and yellowish brown (Sy-) soil horizons indicating repeated Ub-Td soil formation phases relating to variable climate through the Quaternary. Both successions are punctuated by the occurrence of rhyolitic tephra horizons (indicated in red) sourced from the central North Island that have provided independent chronological control. Such successions with chrononological tie-points facilitate direct correlation to the marine oxygen isotope records (e.g. Pillans, 2017 and refs. above) that would otherwise be based on relative age constraints and counting paleosol-loess couplets back from present day. These western North Island multisequal soil successions have strong morphological resemblance with those andic soil successions occurring in southern continental Chile overlying Quaternary-aged glacial and glacio-fluvial landforms. (For interpretation of the references to colour in this figure legend, the reader is referred to the Web version of this article.)
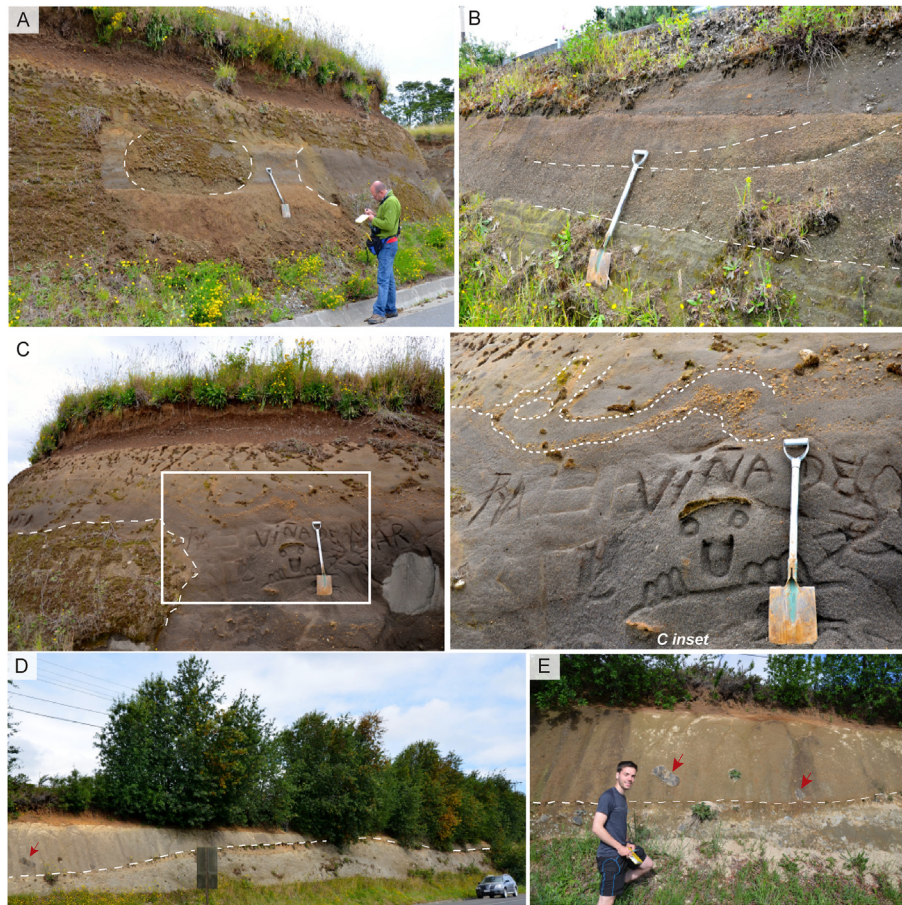
Fig. 8. A—C. Non-cohesive volcanic mass-flow deposits are frequently associated with drift and outwash deposits in northwest Patagonia. At Puente Minte, ~6.7 km east of Puerto Varas (41°18′ 50.9′ S, 72°53′ 38.7′ W), multiple late last glacial aged debris-hyperconcentrated flow deposits sourced from an ancestral Calbuco Volcano have widely inundated glaciated surfaces bordering Lago Llanquihue, as well as eroded into pre-existing glacial and volcaniclastic deposits. Inset C shows highly irregular pumice layers entrained within a channelized debris flow deposit; D, E. At Puente Negro on Ruta 5, ~2.8 km north of the Puerto Montt Peaje (41°24′ 48.3′S, 72°57′ 26.6′W) a massive to weakly stratified debris-flow deposit containing pumice clasts and bread-crusted bombs can be observed to surmount and thin out over adjacent and more elevated LGM-aged moraines.

and Michimahuida volcanoes in the Chaitén sector have been recognised beyond this limit (Alloway et al. 2017a, b) but are confined to post-glacial aged uppermost andic soil material (Sr1). In the vicinity of Puerto Montt Hospital (41°26′54.2″S, 72°57′19.5″W), an older prominent weathered tephra can be identified in a woody lignite sequence occurring between two glacio-fluvial outwash deposits of LGM and pre-LGM (>45 ^{14}C ka BP) age. Two radiocarbon dates of 45,600 ± 2500 ^{14}C a BP (UCIAMS-145967; lignite) and 45,700 ± 2500 ^{14}C a BP (UCIAMS-145932; wood) from immediately beneath this tephra establish a maximum age (see Fig. 10A—C). Such exposures revealing tephra of this antiquity are rare in this region and this same tephra has yet to be recognised elsewhere within equivalent-aged andic soils or organic-rich sediments.

6. Vegetation and climate record

Palynological investigations on ODP Site 1233 (41°0.005 S, 74°26.992 W, 838-m water depth) and the Taiquemó bog (42.17°S, 73.60°W) on Isla Grande de Chiloé (see Fig. 11) yielded continuous, well-dated records of vegetation change through the last glacial-interglacial cycle in northwest Patagonia (Heusser, 1990, 2003; Heusser et al., 2006; Heusser and Heusser, 2006). Significantly, the palynology of ODP 1233 extends continuously over the last 93,000 years, spanning from MIS 5b to the present.

These records show similar trends through MIS 3 with a preponderance of cold-resistant southern beech (*N. dombeyi* type), conifers (*Pilgerodendron*, *Podocarpus nubigena*) and Poaceae, indicating a subantarctic woodland under cold and humid conditions. Poaceae increased during MIS 2 (between ~30 and ~17 cal ka BP) at the expense of *Nothofagus,* suggesting the establishment of a subantarctic parkland under extreme glacial conditions, followed by the spread of thermophilous trees (Myrtaceae, *Lomatia*) and ferns (*Lophosoria*) characteristic of north Patagonian rainforests at ~17.8 cal ka BP. This warming event marks the beginning of the last glacial termination and led to the establishment of closed canopy rainforests in the mainland of the Chilean Lake District and Isla Grande de Chiloé (Moreno et al., 2015; Pesce and Moreno, 2014). Subsequent warming and decline in precipitation led to the expansion of Valdivian rainforests during the early Holocene, followed by a cooling trend and increased precipitation commencing at 7.8 cal ka BP. Centennial-scale variability started at ~6 ka and led to the establishment of a mosaic of north Patagonian and Valdivian rainforest communities that persist until the present (Moreno and Videla, 2016).

Remarkable in the ODP1233 record is the abundance and continuous presence of arboreal pollen (*Nothofagus)* during the last glaciation with a mean of ~60% (MIS5 b to MIS 2), accompanied by relatively modest abundance of herbs (Poaceae, 20%), other trees
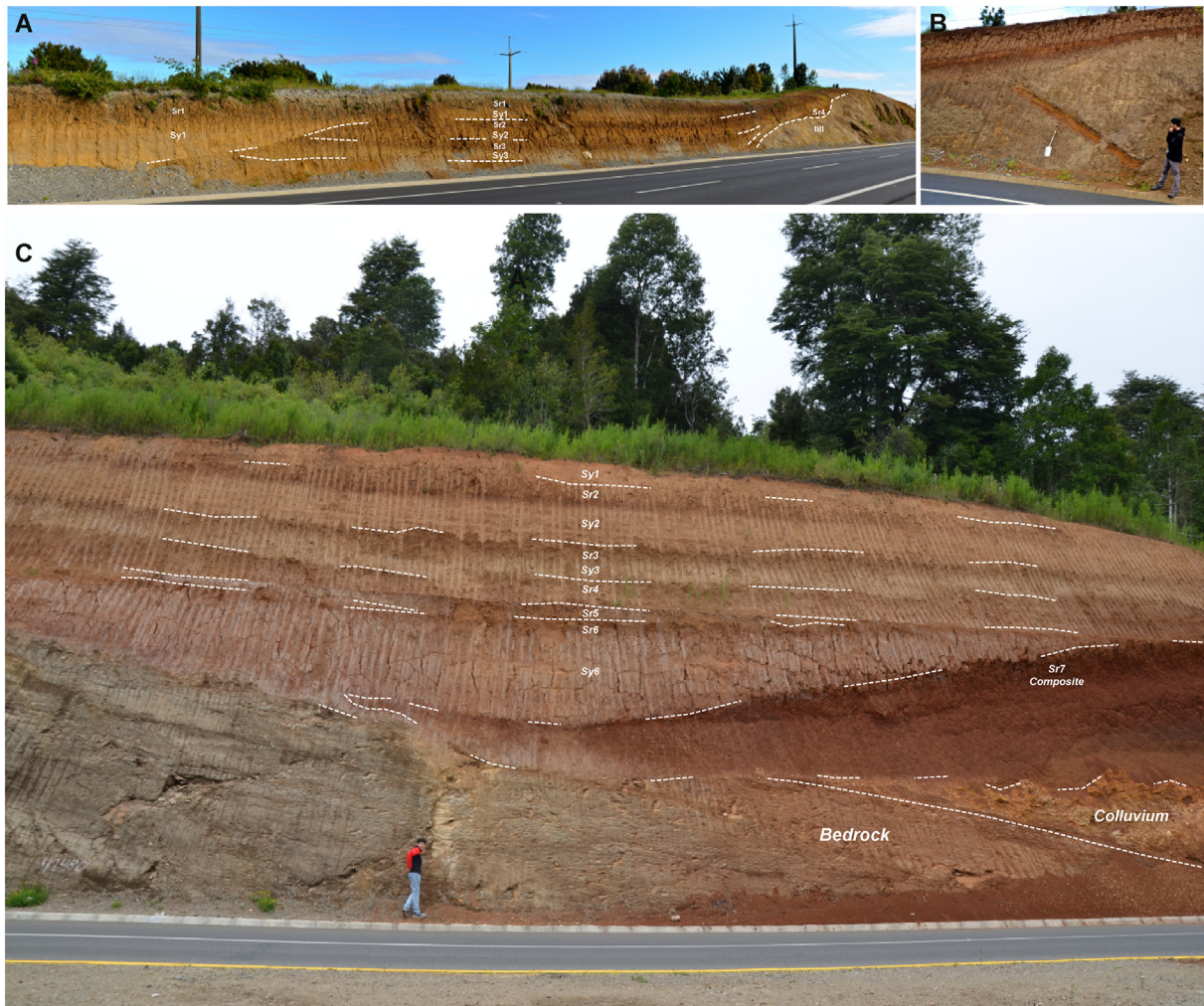
Fig. 9. A, B. Road section on Ruta 5 (road-marker km-1054.2) between Puerto Montt and Pargua, and 0.8 km south of Peaje Puente Tenéo (41°37′ 25.0′S; 73°16′ 46.9′W) showing a multisequal soil succession with four Sr-Sy couplets overlying a highly-weathered glacial diamict (till) with a ~4.2-m-long, large diameter (>1-m) tree-trunk mold encased within its matrix. Note the localised cross-cutting relationship of Sy1 truncating older soil horizons and clearly indicating pedospheric stripping. Laterally (southwards) along section, Sy1 becomes conformable with underlying soil horizons. C. Road section exposed in the vicinity of north Valdivia on Ruta 205 and 200-m south from the T-344 junction to Las Marias (39°45′ 51.6′ S; 73°13′ 41.0′W). Here, six Sr-Sy couplets are conspicuously exposed overlying a very prominent >3 m-thick composite paleosol developed on a colluvium wedge resting on bedrock. This succession provides clear indication that layered soil sequences reflecting multiple *Ub-Td* soil forming cycles have developed under varying paleoenvironmental conditions and are likely (but yet to be proven) formed over a much longer timeframe than those soil sequences observed further south. This section is important in that multisequal soil successions can be clearly recognised in other regions of southern Chile less affected by the direct influence of piedmont glaciation. A majority of soil sections in the vicinity of Valdivia typically reveal a prominent well-developed reddish soil typically resting on bedrock with little to negligible horizon differentiation. Such an undifferentiated profile develops in response to low to negligible accretionary flux of wind-borne materials, which over time, results in the formation of a thick-topdown overprinted composite soil similar to that composite paleosol which is evident at the bottom of the north Valdivia roadside profile.

and herbs. *Nothofagus* abundance in the Taiquemó mire was higher (~80%) than ODP1233 between ~50 and 30 ka (MIS 3) and similar between 30 and 18 cal ka BP (MIS 2—60%), though more variable. The Taiquemó mire, which was located a few kilometres from MIS 2 moraines and a few metres west from MIS 4 glacial margins, indicates a continuous cover of predominantly arboreal vegetation during the coldest episodes of the last glaciation. These results suggest that even under extreme glacial temperature, precipitation and windiness (katabatic winds at the western end of the Golfo de Ancud ice lobe) ice-free areas in the lowlands of northwest Patagonia were vegetated by subantarctic parkland and/or scattered woodland. These conditions may have suppressed aeolian entrainment of sand or finer particles from the extensive, well-drained and active outwash plain surfaces during stadial and interstadial episodes of the last glaciation.
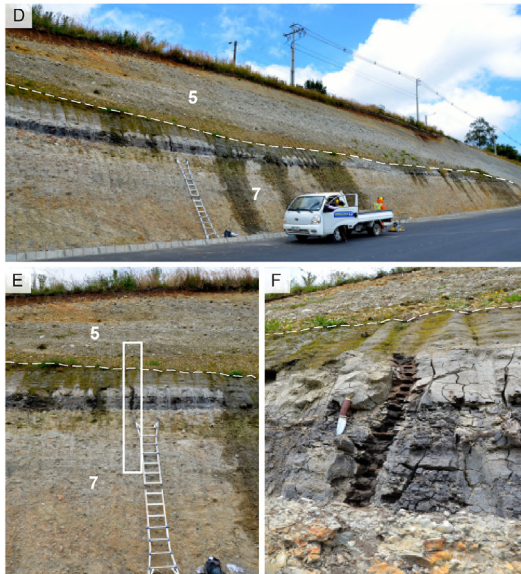
7. Discussion and conclusions

Here, we make a case that multisequal soil successions in northwest Patagonia provide a relatively untapped archive to reconstruct Quaternary glacial and environmental changes. Patagonia contains a geomorphic record of glaciations going back well into the Quaternary Period, and a glacial stratigraphic record as old as Miocene in age (Mercer, 1976). On the eastern, more arid, side of the Andes, cosmogenic dating (as well as OSL and K-Ar, ^{40}Ar/^{39}Ar) of moraines and outwash plains (Fig. 12), has revealed insight into glaciations older than the last glacial cycle, to perhaps > Stage 6 time (>130 ka), stage 8 (~200—300 ka), and as old as 1 Ma (e.g., Singer et al., 2004; Kaplan et al., 2005; Hein et al., 2009; 2017). However, using these same approaches, dating glaciations older than the LGM has been problematic, if not impossible on the wet western side of the Andes (Fig. 4) due to persistent vegetation cover
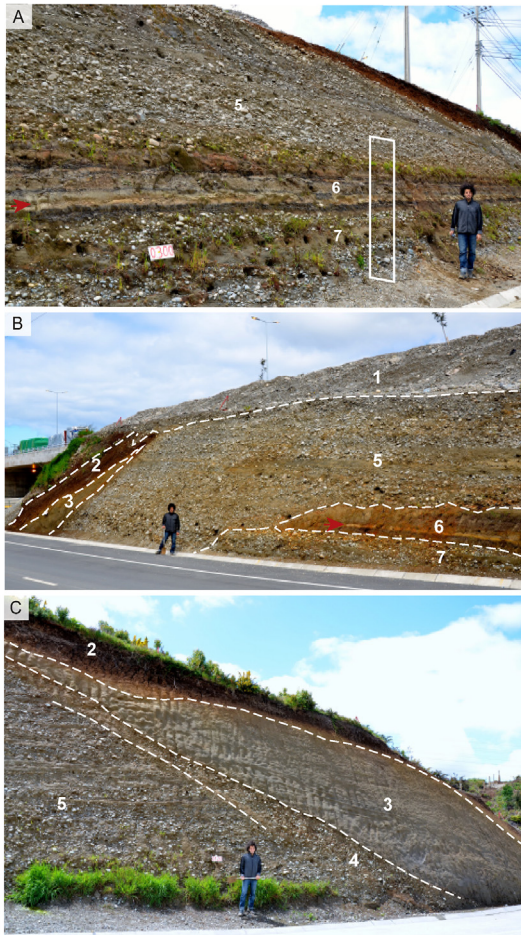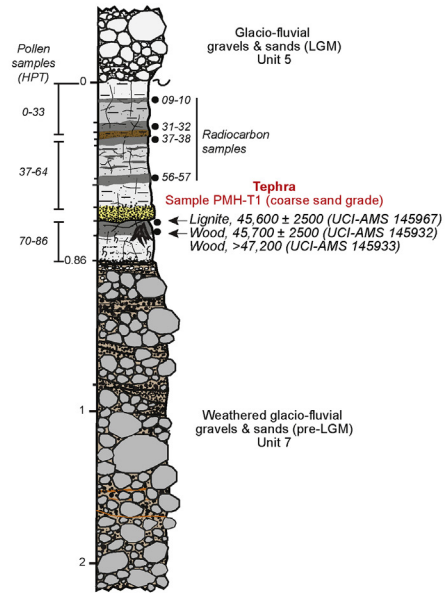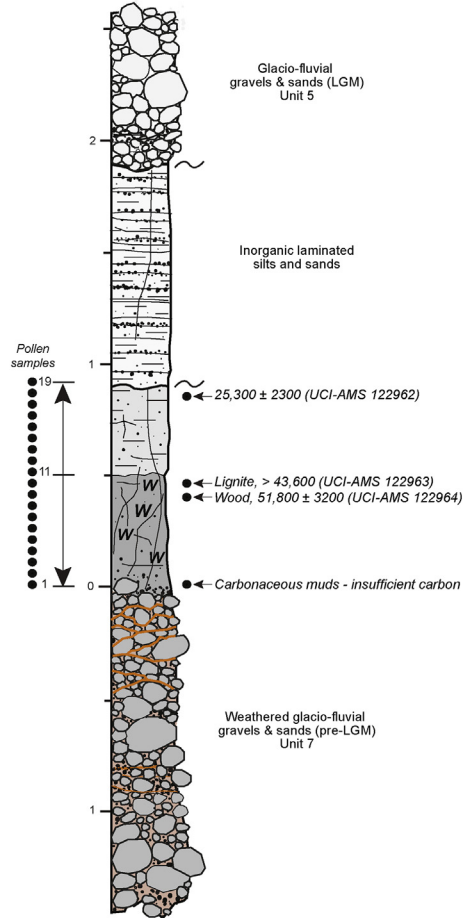
KEY

1   Fill
2   Andic soil material (post-glacial)
3   Volcanigenic hyperconcentrated flow (hcf) deposit
4   Colluvium
5   Glacio-fluvial gravels & sands (LGM)
6   Truncated carbonaceous mud sequence containing a prominent tephra and wood in growth position
7   Weathered glacio-fluvial gravels & sands (pre-LGM)
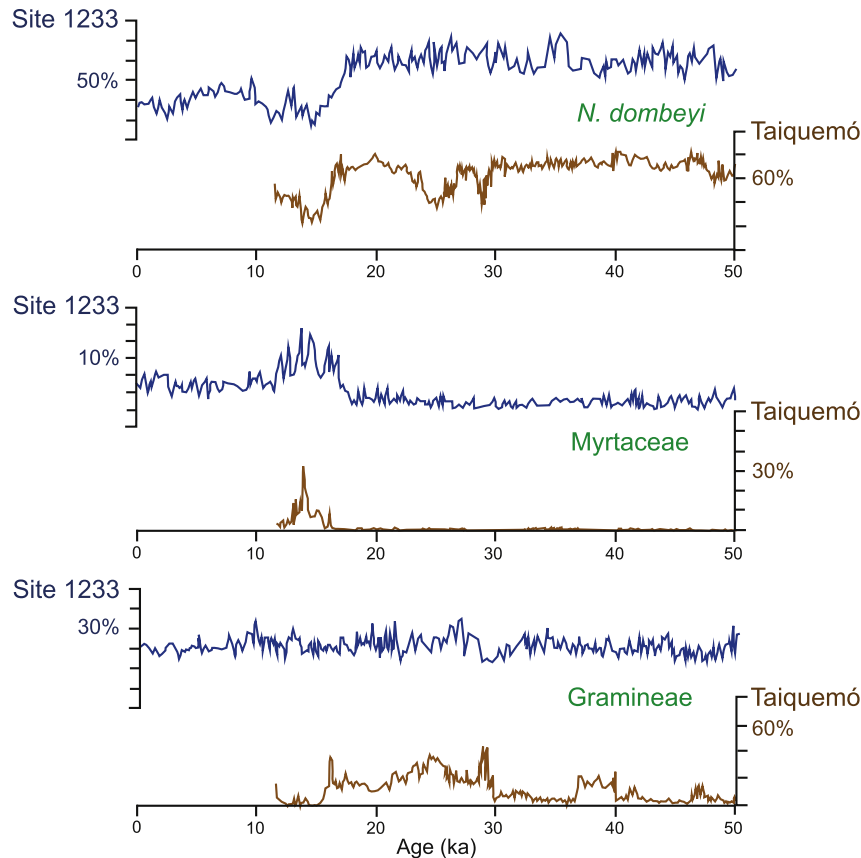
Puerto Montt Hospital Overpass
west-facing road section
S 41° 26' 54.2"
W 72° 57' 19.5"

Glacio-fluvial gravels & sands (LGM) Unit 5

Pollen samples (HPT)

0-33

09-10
31-32   *Radiocarbon*
37-38   *samples*

37-64

56-57

Tephra
Sample PMH-T1 (coarse sand grade)

70-86

◄— *Lignite, 45,600 ± 2500 (UCI-AMS 145967)*
◄— *Wood, 45,700 ± 2500 (UCI-AMS 145932)*
Wood, >47,200 (UCI-AMS 145933)

Weathered glacio-fluvial gravels & sands (pre-LGM) Unit 7

Pargua-Puerto Montt Highway
west-facing road section
11.5 km south of Huelmo turnoff,
3.6 km north of Calbuco over-pass
S 41° 34' 25.4"
W 73° 12' 05.2"

Glacio-fluvial gravels & sands (LGM) Unit 5

Inorganic laminated silts and sands

Pollen samples

19

◄— *25,300 ± 2300 (UCI-AMS 122962)*

11

◄— *Lignite, > 43,600 (UCI-AMS 122963)*
◄— *Wood, 51,800 ± 3200 (UCI-AMS 122964)*

◄— *Carbonaceous muds - insufficient carbon*

Weathered glacio-fluvial gravels & sands (pre-LGM) Unit 7

Fig. 11. Comparison of *N. dombeyi,* Myrtaceae and Gramineae pollen spectra from ODP Site 1233 (41°0.005 S, 74°26.992 W, 838-m water depth) and Taiquemó mire (42.17° S, 73.60° W) on Isla Grande de Chiloé (*modified from* Heusser et al., 2006) provide a continuous ~50,000-yr record of regional changes in vegetation from southern Chile, and provides key information on prevailing paleoenvironmental conditions and persistence of vegetation during equivalent-aged *Ub-Td* soil formation cycles. Note the continuous presence and abundance of arboreal pollen (*Nothofagus*).

during both glacial and post-glacial times, as well as widespread inundation of glacial drift and associated outwash deposits by volcanic mass-flows.
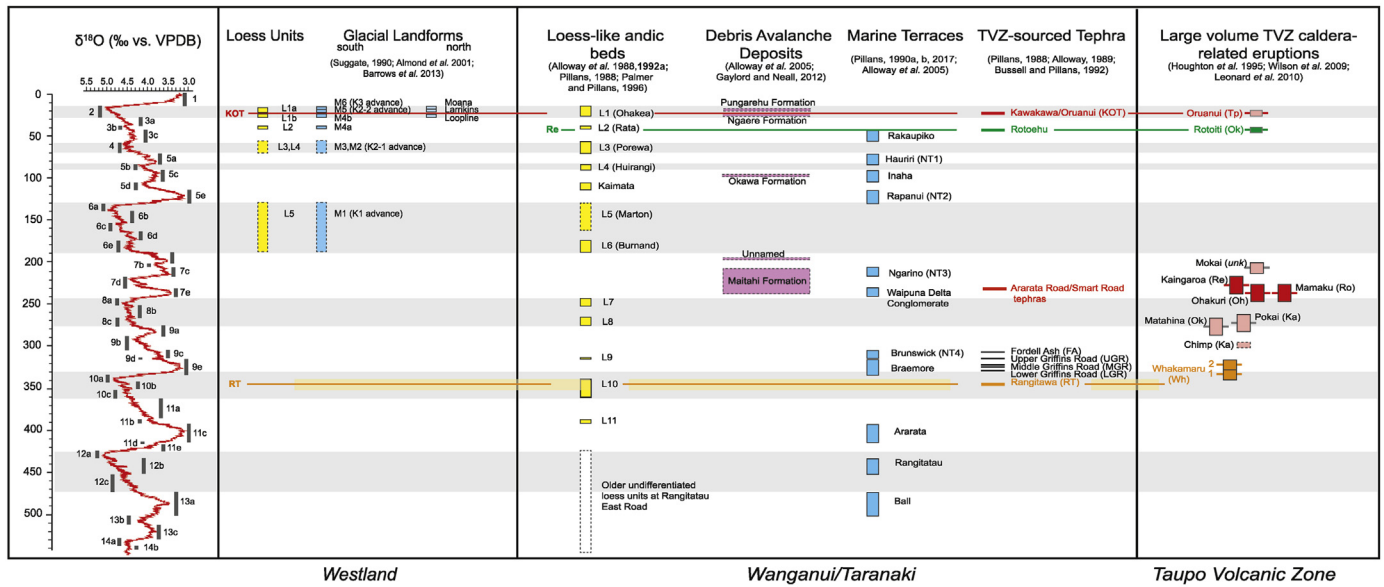
In New Zealand, at a similar southern mid-latitude position to northwest Patagonia, an increasing number of soil horizons is recognised on successively older Quaternary-aged landforms (Fig. 12A). In South Westland, this relationship has been demonstrated for successively older moraines and associated outwash surfaces, while in Taranaki and Wanganui regions of western North Island this has been similarly demonstrated for successively older marine and fluvial terraces. These multisequal soil successions have been related to coupled phases of topdown and upbuilding soil formation associated with fluctuating cycles of interglacial/warm and stadial/cold climate respectively, following stabilisation of the landform on which the soils accumulated. Based on soil genesis analogues from New Zealand, we propose a similar soil-stratigraphic model for cover-bed sequences in southern continental Chile (see Fig. 12B). Up to four sets of coupled Sr- and Sy-horizons reflecting four sequential cycles of Ub-Td soil formation can be observed overlying glacial drift and outwash deposits in southern continental Chile. Northwards in the vicinity of Valdivia (~40°S) even thicker successions occur with greater number of

coupled Sr- and Sy-horizons (Fig. 9C). The basal ages of these coupled Valdivian soil sequences are unknown but there exists the opportunity to link via cover-bed sequences to dated marine terraces preserved along the coast of this region (e.g. Fuenzalida et al., 1965; Antinao and McDonough, 1999; Pino et al., 2002; Jara-Muñoz et al., 2015) in an approach similar to that undertaken for New Zealand marine terrace sequences (e.g. Pillans, 1983, 1990a; 1990b, 2017; Berryman, 1992; Alloway et al., 2005; Wilson et al., 2007).
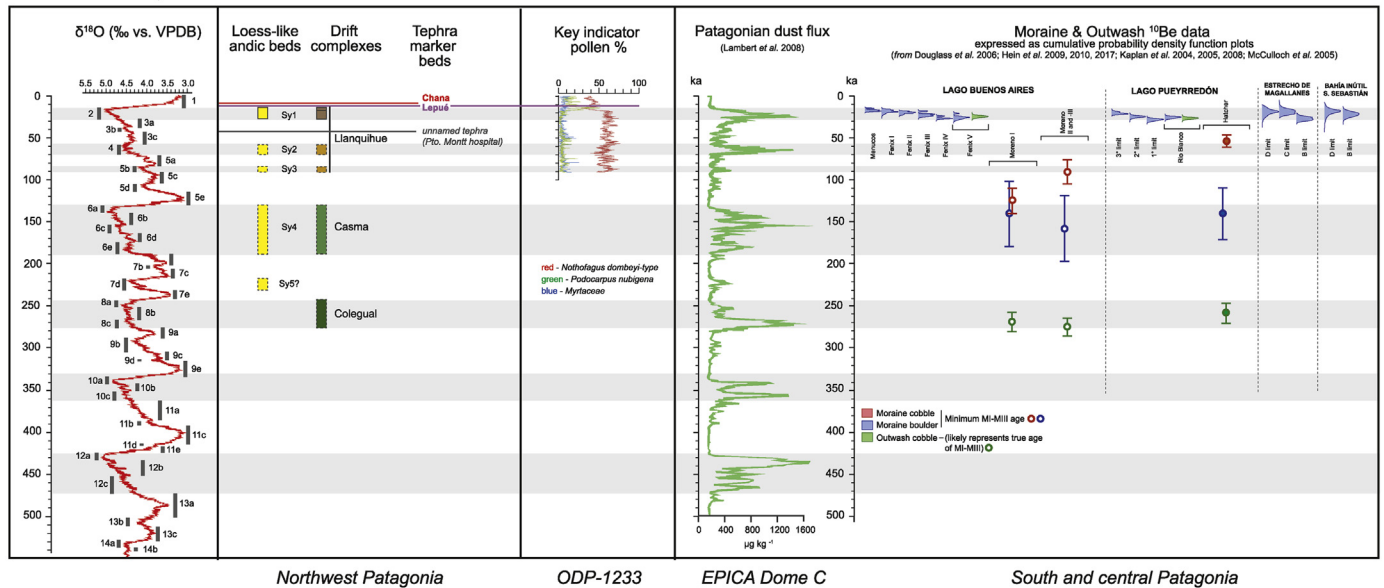
The paucity of widespread loess in southern continental Chile despite the proximity of extensive piedmont glaciation and associated outwash surfaces seems perplexing but this likely indicates that prevailing environmental conditions tended to suppress both the formation and restrict the widespread mobilisation of loess in this landscape. Palynological analysis from equivalent-aged terrestrial and marine sediments during MIS 3 and 2 indicate near-continuous vegetation ground cover (scattered *Nothofagus* woodland) under conditions of high precipitation and variable temperature and windiness (Fig. 11). Clearly the analysis of older (>MIS-3) terrestrial palynological records will be essential for assessing vegetation associations as well as their persistence through earlier glacial/interglacial cycles. Unfortunately, such records in northwest Patagonia are both fragmentary and rare.

Fig. 10. A—C. In the vicinity of Puerto Montt Hospital (41°26′54.2″S, 72°57′19.5″W), a prominent weathered tephra is preserved within a woody lignite sequence intervening between two glacio-fluvial outwash deposits of LGM and pre-LGM (>45 ^{14}C ka BP) age. The upper (LGM) glacio-fluvial sediments are deeply incised with colluviated channel margins partially surmounted and veneered by a prominent volcanic hyperconcentrated flow deposit. The entire sequence is mantled by andic soil material of late last glacial to post-glacial age; D-F. An equivalent-aged sequence can be observed on Ruta 5 south of Puerto Montt (41°34′25.4″S, 73°12′05.2″W) Here, woody lignites intervene between LGM glacio-fluvial outwash deposits above and pre-LGM till below. Such sections in northwest Patagonia are rarely exposed.

Fig. 12. A. Correlation summary (upper panel) of cover-bed deposits and associated landforms from western and central regions of New Zealand, including Westland (Suggate, 1990; Almond, 1996; Almond and Tonkin, 1999; Almond et al., 2001; Barrows et al., 2013), Wanganui-Taranaki (Alloway, 1989; Alloway et al., 1988, 1992a, 2005; Bussell and Pillans, 1992; Gaylord and Neall, 2012 Palmer and Pillans, 1996; Pillans, 1983, 1988, 1990a,b, 2017; Pillans et al., 1993, 1996) and Taupo Volcanic Zone (TVZ) extending over the last 0.5 Myrs (e.g. Houghton et al., 1995; Wilson et al., 2009; Leonard et al., 2010). Dated tephra marker beds (e.g. Pillans et al., 1996; Danišík et al., 2012; Vandergoes et al., 2013) sourced from the TVZ occurring within these regions are indicated as coloured horizontal lines with 1-SD indicated; B. Correlation summary (lower panel) from Patagonia, South America, indicates 'loess-like' andic deposits *(this study)*, glacial drift (Andersen et al., 1999; Denton et al., 1999a,b) and intervening tephra marker beds (Alloway et al., 2017a, b) from northwest Patagonia, key pollen percentages from ODP-1233 (red - *Nothofagus dombeyi*-type, green − *Podocarpus nubigena,* and blue − *Myrtaceae*), Patagonian dust flux data from EPICA Dome C, Antarctica (from Lambert et al., 2008) and moraine boulder and outwash cobble [10]Be data from south and central Patagonia are included for comparative purposes. LGM and Late Glacial [10]Be data are expressed as cumulative probability density function plots *(from* Douglass et al., 2006; Hein et al., 2009, 2010, 2017; Kaplan et al., 2004, 2005, 2008; McCulloch et al. 2005). In contrast, for those (Pre-LGM) moraine systems that exhibit a large spread on their ages, we include the mean value for the landform (±1σ including a 3% production-rate uncertainty propagated) following those in original publications. Also, following Hein et al. (2009) and Hein et al. (2017), we infer the ages from pre-LGM outwash plains more likely represent the true age of the landform (±1σ). That is, in the case of the Moreno I and Moreno II-III moraines (in Lago Buenos Aires), and Hatcher moraines (in Lago Pueyrredón), we suggest that the moraine boulders and cobbles yielded minimum ages for the landform; the outwash cobble ages likely represent a more accurate age for the entire moraine-outwash complexes. The MIS data are the LR04 stack of Lisiecki and Raymo (2005), while the scheme of lettered marine isotope substages is from Railsback et al. (2015). (For interpretation of the references to colour in this figure legend, the reader is referred to the Web version of this article.)

Observed multisequel soils cannot be simply explained by coupled soil formation phases of enhanced upbuilding (Ub > Td) by glacially derived wind-borne sediment during full glacial and cool climate episodes and intensified topdown pedogenesis (Td > Ub) during interglacial and/or warm climate episodes. Rather, coupled Sr- and Sy-horizons (reflecting a Td-Ub cycle) are formed by continuous addition of intermittently erupted Andean-sourced tephra deposited to the ground surface during different climatic episodes - Sr-horizons reflecting enhanced topdown soil formation during interglacial and warm interstadials, and Sy-horizons

reflecting reduced topdown soil formation during full glacial and cool stadials, i.e. developmental upbuilding. The colour and structure is a direct reflection of differential weathering under different climate regimes but also may be attributed to differences in Al:Si ratio of the nanocrystalline materials which have been related to mean annual rainfall and the level of Si and Fe in soil solution (Parfitt et al., 1983; Alloway et al., 1992b,c; Churchman and Lowe, 2012).

The recognition of multisequal soil successions in southern continental Chile and their implied connection to variations in Quaternary climate presents a tantalising opportunity for researchers to identify magnetic excursions (e.g. Blake excursion, ~115–122 ka; Icelandic basin excursion, ~190 ka; see Thorveny et al., 2004) within these cover-bed sequences as well as conduct luminescence dating in order to firmly link these layers with variations indicated from the established oxygen isotope record. Ultimately, our stratigraphic approach, which includes an appreciation of the critical role of upbuilding pedogenesis (cf. 'classical' topdown pedogenesis), will enable us to better constrain the age of this well-preserved sequence of Andean-sourced drift and outwash deposits, the older members of which are difficult to differentiate by morphostratigraphic means and which all lie near or beyond the current limits of radiocarbon dating.

Acknowledgements

Appendix A. Supplementary data

Supplementary data related to this article can be found at https://doi.org/10.1016/j.quascirev.2018.04.005.

References

Alloway, B.V., 1989. Late Quaternary Cover-bed Stratigraphy and Tephrochronology of North-eastern and Central Taranaki, New Zealand. Unpublished Ph.D. thesis. lodged in the Library, Massey University, Palmerston North.

Alloway, B.V., Neall, V.E., Vucetich, C.G., 1988. Localised volcanic loess deposits in north Taranaki, New Zealand. In: Eden, Furkert, A.A. (Eds.), Loess - its Distribution, Geology and Soils. Balkema Publishers, Rotterdam, pp. 1–6.

Alloway, B.V., Stewart, R.B., Neall, V.E., Vucetich, C.G., 1992a. Climate of the Last Glaciation in New Zealand, based on aerosolic quartz influx in an andesitic terrain. Quat. Res. 38, 170–179.

Alloway, B.V., Neall, V.E., Vucetich, C.G., 1992b. Particle size analyses of late Quaternary allophane-dominated andesitic deposits from New Zealand. Quat. Intl. 13/14, 167–174.

Alloway, B.V., McGlone, M.S., Neall, V.E., Vucetich, C.G., 1992c. The role of Egmont-sourced tephra in evaluating the paleoclimatic correspondence between the bio- and soil-stratigraphic records of central Taranaki. Quat. Intl. 13/14, 187–194.

Alloway, B.V., Neall, V.E., Vucetich, C.G., 1995. Late Quaternary tephrostratigraphy of northeast and central Taranaki, New Zealand. J. Roy. Soc. N. Z. 25, 385–458.

Alloway, B.V., McComb, P., Neall, V.E., Vucetich, C.G., Gibb, J.G., Sherburn, S., Stirling, M., 2005. Stratigraphy, age and correlation of voluminous debris avalanche events from an ancestral Egmont Volcano: implications for coastal plain construction and regional hazard assessment. J. Roy. Soc. N. Z. 35, 229–267.

Alloway, B.V., Lowe, D.J., Barrell, D.J.A., Newnham, R.M., Almond, P.C., Augustinus, P.C., Bertler, N.A.N., Carter, L.C., Litchfield, L.C., McGlone, M.S., Shulmeister, J., Vandergoes, M.J., Williams, P.W., NZ-INTIMATE Members, 2007. Towards a climate event stratigraphy for New Zealand over the past 30,000 years. J. Quat. Sci. 22, 9–35.

Alloway, B.V., Pearce, N.J., Villarosa, G., Outes, V., Moreno, P.I., 2015. Multiple melt bodies fed the AD 2011 eruption of Puyehue-Cordón Caulle, Chile. Nature Scient. Rept. 5, 17589. https://doi.org/10.1038/srep17589.

Alloway, B.V., Pearce, N.J.G., Moreno, P.I., Villarosa, G., Jara, I., Ricardo De Pol-Holz, R., Outes, V., 2017a. An 18,000 year-long eruptive record from Volcán Chaitén, northwestern Patagonia: paleoenvironmental and hazard-assessment implications. Quat. Sci. Rev. 168, 151–181.

Alloway, B.V., Moreno, P.I., Pearce, N.J.G., De Pol-Holz, R., Henríquez, W., Pesce, O., Sagredo, E., Villarosa, G., Outes, V., 2017b. Stratigraphy, age and correlation of Lepué Tephra: a widespread c. 11,000 cal. a BP marker horizon sourced from the Chaitén Sector of southern Chile. J. Quat. Sci. 32, 795–829.

Andersen, B.G., Denton, G.H., Lowell, T.V., 1999. Glacial geomorphologic maps of the Llanquihue drift in the area of the southern Lake District, Chile. Geografiska Annaler Series A Physical Geography 81A, 155–166.

Antinao, J.L., McDonough, M., 1999. Antecedentes estratigráficos y geochronológicos para una edad interglacial (MIO5e–5c) de las terraza pleistocena de 'Cancagua'. In: Valdivia, Chile. XIV Congreso Geologico Argentino, Actas I: 55-56.

Almond, P.C., 1996. Loess, soil stratigraphy and Aokautere Ash on late Pleistocene surfaces in south Westland, New Zealand: interpretation and correlation with the glacial stratigraphy. Quat. Int. 13/14, 163–176.

Almond, P.C., Tonkin, P.J., 1999. Pedogenesis by upbuilding in an extreme leaching and weathering environment, and slow loess accretion, South Westland, New Zealand. Geoderma 92, 1–36.

Almond, P.C., Moar, N.T., Lian, O.B., 2001. Reinterpretation of the glacial chronology of south Westland, New Zealand. New Zealand Journal of Geology and Geophysics 44, 1–15.

Balco, G., Stone, J.O., Lifton, N.A., Dunai, T.J., 2008. A complete and easily accessible means of calculating surface exposure ages or erosion rates from Be-10 and Al-26 measurements. Quat. Geochronol. 3, 174–195.

Barrell, D.J.A., Almond, P.C., Vandergoes, M.J., Lowe, D.J., Newnham, R.M., NZ-INTIMATE Members, 2013. A composite pollen-based stratotype for interregional evaluation of climatic events over the past 30,000 years (NZ-INTIMATE project). Quat. Sci. Rev. 74, 4–20.

Barrows, T.T., Almond, P., Rose, R., Fifield, K.L., Mills, S.C., Tims, S.G., 2013. Late pleistocene glacial stratigraphy of the Kumara-Moana region, West Coast of south island, New Zealand. Quat. Sci. Rev. 74, 139–159.

Berger, G.W., Almond, P.C., Pillans, B.J., 2001a. Luminescence dating and glacial stratigraphy in Westland, New Zealand. New Zealand Journal of Geology and Geophysics 44, 25–35.

Berger, G.W., Pillans, B.J., Tonkin, P.J., 2001b. Luminescence chronology of loess-paleosol sequences in Canterbury, South Island, New Zealand. New Zealand Journal of Geology and Geophysics 44, 501–516.

Berger, G.W., Pillans, B.J., Bruce, J.G., McIntosh, P.D., 2002. Luminescence chronology of loess-paleosol sequences from southern South Island, New Zealand. Quat. Sci. Rev. 21, 1899–1913.

Berryman, K., 1992. A stratigraphic age of Rotoehu Ash and late Pleistocene climate interpretation based on marine terrace chronology, Mahia Peninsula, North Island, New Zealand. New Zealand Journal of Geology and Geophysics 35, 1–7.

Bruce, J.G., 1973. Pedology of some soils on loess in Southland and Otago, New Zealand. New Zealand Journal of Science 16, 333–347.

Bruce, J.G., 1996. Morphological characteristics and interpretation of some polygenetic soils in loess in southern South Island, New Zealand. Quat. Int. 34–36, 205–211.

Bussell, M.R., Pillans, B.J., 1992. Vegetational and climatic history during oxygen isotope stage 9, Wanganui district, New Zealand, and correlation of the Fordell Ash. J. Roy. Soc. N. Z. 22, 41–60.

Caldenius, C., 1932. Las Glaciaciones Cuaternarias en Patagonia y Tierra del Fuego. Ministerio de Agricultura de la Nación. Dirección General de Minas y Geologia 95 (1), 148.

Carter, J.A., Lian, O.B., 2000. Palaeoenvironmental reconstruction from the last interglacial using phytolith analysis, southeast North Island, New Zealand. J. Quat. Sci. 15, 733–743.

Casanova, M., Salazar, O., Seguel, O., Luzio, W., 2013. The Soils of Chile. World Soils Book Series. Springer Netherlands, p. 185.

Churchman, G.J., Lowe, D.J., 2012. Alteration, formation, and occurrence of minerals in soils. Properties and Processes. In: Huang, P.M., Li, Y., Sumner, M.E. (Eds.), Handbook of Soil Sciences, second ed., vol. 1. CRC Press, Boca Raton, FL, pp. 20.1–20.72.

Clayden, B., Hewitt, A.E., 1994. Horizon Notation for New Zealand Soils. Manaaki Whenua Press, New Zealand. ISBN 047804528X.

Cox, S.C., Barrell, D.J.A., (compilers), 2007. Geology of the Aoraki area: scale 1: 250,000. Lower Hutt: GNS Science. Institute of Geological & Nuclear Sciences, 1: 250,000 geological map 15, 71 p. + 1 folded map.

Danišík, M., Shane, P.A.R., Schmitt, A.K., Hogg, A.G., Santos, G.M., Storm, S.,

Evans, N.J., Fifield, L.K., Lindsay, J.M., 2012. Re-anchoring the late Pleistocene tephrochronology of New Zealand based on concordant radiocarbon ages and combined 238U/230Th disequilibrium and (U-Th)/He zircon ages. Earth Planet Sci. Lett. 349–350, 240–250.

Denton, G.H., Heusser, C.J., Lowell, T.V., Moreno, P.I., Andersen, B.G., Heusser, L.E., Schlüchter, C., Marchant, D.R., 1999a. Inter-hemispheric linkages of paleo-climate during the last glaciation. Geogr. Ann. 81A, 107–153.

Denton, G.H., Lowell, T.V., Heusser, C.J., Schlüchter, C., Andersen, B.G., Heusser, L.E., Moreno, P.I., Marchant, D.R., 1999b. Geomorphology, stratigraphy and radio-carbon chronology of Llanquihue drift in the area of the Southern Lake District, Seno Relongcaví and Isla Grande de Chiloé, Chile. Geogr. Ann. 81A, 167–229.

Douglass, D.C., Bockheim, J.G., 2006. Soil-forming rates and processes on quaternary moraines near Lago Buenos Aires, Argentina. Quat. Res. 65, 293–307.

Douglass, D.C., Singer, B.S., Kaplan, M.R., Mickelson, D.M., Caffee, M.W., 2006. Cosmogenic nuclide surface exposure dating of boulders on last-glacial and late-glacial moraines, Lago Buenos Aires, Argentina: interpretive strategies and paleoclimate implications. Quat. Geochronol. 1, 43–58.

Dunbar, N.W., Iverson, N.A., Van Eaton, A.R., Sigl, M., Alloway, B.V., Kurbatov, A.V., Mastin, L.G., McConnell, J.R., Wilson, C.J.N., 2017. New Zealand super-eruption provides time marker for the Last Glacial Maximum in Antarctica. Nature Scientific Reports 7, 12238. https://doi.org/10.1038/s41598-017-11758-0.

Eden, D.N., 1989. River terraces and their loessial cover beds, awatere river valley, South Island, New Zealand. New Zealand Journal of Geology and Geophysics 32, 487–497.

Eden, D.N., Hammond, A.P., 2003. Dust accumulation in the New Zealand region since the last glacial maximum. Quat. Sci. Rev. 22, 2037–2052.

Eger, A., Almond, P.C., Condron, L.M., 2011. Pedogenesis, soil mass balance, phosphorus dynamics and vegetation communities across a Holocene soil chronosequence in a super-humid climate, South Westland, New Zealand. Geoderma 163, 185–196.

Eger, A., Almond, P.C., Condron, L.M., 2012. Upbuilding pedogenesis under active loess deposition in a super-humid, temperate climate — quantification of deposition rates, soil chemistry and pedogenic thresholds. Geoderma 189–190, 491–501.

Eger, A., Almond, P.C., Condron, L.M., 2013. Phosphorus fertilisation by active Holocene dust deposition in a super-humid, temperate environment (West Coast, South Island, New Zealand) — soil phosphorus fractionation and accession processes. Global Biogeochem. Cycles 27, 108–118.

FAO-UNESCO, 1971. South America. Soil Map of the World, vol. IV. UNESCO, Paris.

Fontijn, K., Lachowycz, S.M., Rawson, H., Pyle, D.M., Mather, T.A., Naranjo, J.A., Moreno-Roa, H., 2014. Late Quaternary tephrostratigraphy of southern Chile and Argentina. Quat. Sci. Rev. 89, 70–84.

Fuenzalida, H.V., Cooke, R., Paskoff, R., Segerstrom, K., Wolfgang Weischet, W., 1965. High stands of quaternary sea level along the Chilean coast. International Studies on the Quaternary. In: Wright Jr., H.E., Frey, D.G. (Eds.), International Studies on the Quaternary: Papers Prepared on the Occasion of the VII Congress of the International Association for Quaternary Research, Boulder, Colorado; Special Paper of the Geological Society of America, vol. 84, pp. 473–496.

Gaylord, D.R., Neall, V.E., 2012. Subedifice collapse of an andesitic stratovolcano: the Maitahi formation, Taranaki peninsula, New Zealand. Geol. Soc. Am. Bull. 124, 181–199.

Goh, K.M., Tonkin, P.J., Rafter, T.A., 1978. Implications of improved radiocarbon dates of Timaru peats on Quaternary loess stratigraphy. New Zealand Journal of Geology and Geophysics 21, 463–466.

Hein, A.S., Hulton, N.R., Dunai, T.J., Schnabel, C., Kaplan, M.R., Naylor, M., Xu, S., 2009. Middle Pleistocene glaciation in Patagonia dated by cosmogenic-nuclide measurements on outwash gravels. Earth Planet Sci. Lett. 286, 184–197.

Hein, A.S., Hulton, N.R.J., Dunai, T.J., Sugden, D.E., Kaplan, M.R., Xu, S., 2010. The chronology of the last glacial maximum and deglacial events in central argentine Patagonia. Quat. Sci. Rev. 29, 1212–1227.

Hein, A.S., Cogez, A., Darvill, C.M., Mendelova, M., Kaplan, M.R., Herman, F., Dunai, T.J., Norton, K., Xu, S., Christl, M., 2017. Regional mid-Pleistocene glaciation in central Patagonia. Quat. Sci. Rev. 164, 77–94.

Houghton, B.F., Wilson, C.J.N., Williams, M.O., Lanphere, M.A., Weaver, S.D., Briggs, R.M., Pringle, M.S., 1995. Chronology and dynamics of a large silicic magmatic system: central Taupo Volcanic Zone, New Zealand. Geology 23, 13–16.

Heusser, C.J., 1990. Chilotan piedmont glacier in the southern Andes during the last glacial maximum. Rev. Geol. Chile 17, 3–18.

Heusser, C.J., 2003. Ice Age Southern Andes—A Chronicle of Palaeoecological Events. Elsevier, Amsterdam, p. 240.

Heusser, C.J., Heusser, L.E., Lowell, T.V., 1999. Paleoecology of the southern Chilean Lake District-Isla Grande de Chiloé during middle-Late Llanquihue glaciation and deglaciation. Geogr. Ann. Phys. Geogr. 81A, 231–284.

Heusser, C.J., Heusser, L.E., 2006. Submillennial palynology and palaeoecology of the last glaciation at Taiquemó (~50,000 cal yr, MIS 2–4) in southern Chile. Quat. Sci. Rev. 25, 446–454.

Heusser, L., Heusser, C., Pisias, N., 2006. Vegetation and climate dynamics of southern Chile during the past 50,000 years: results of ODP Site 1233 pollen analysis. Quat. Sci. Rev. 25, 474–485.

Hewitt, A.E., 2010. New Zealand Soil Classification, 3ed Edition. Manaaki Whenua Press, Lincoln, Canterbury, New Zealand, p. 136. ISBN 9780478347104.

Hicks, D.M., Shankar, U., McKerchar, A.I., Basher, L., Jessen, M., Lynn, I., Page, M., 2011. Suspended sediment yields from New Zealand rivers. New Zealand Journal of Hydrology 50, 81–142.

Hughes, M.W., Almond, P.C., Roering, J.J., 2009. Increased sediment transport via bioturbation at last glacial-interglacial transition. Geology 37, 919–922.

Hughes, M.W., Almond, P.C., Roering, J.J., Tonkin, P.J., 2010. Late Quaternary loess landscape evolution on an active tectonic margin, Charwell Basin, South Island, New Zealand. Geomophology 122, 294–308.

Jara-Muñoz, J., Melncik, D., Brill, D., Strecker, M.R., 2015. Segmentation of the 2010 Maule Chile earthquake rupture from a joint analysis of uplifted marine terraces and seismic-cycle deformation patterns. Quat. Sci. Rev. 113, 171–192.

Johnson, D.L., Watson-Stegner, D., 1987. Evolution model of pedogenesis. Soil Sci. 143, 349–366.

Johnson, D.L., Keller, E.A., Rockwell, T.K., 1990. Dynamic pedogenesis: new views on some key soil concepts, and a model for interpreting Quaternary soils. Quat. Res. 33, 306–319.

Kaplan, M., Ackert, R., Singer, B., Douglass, D., Kurz, M., 2004. Cosmogenic nuclide chronology of millennial-scale glacial advances during - isotope stage 2 in Patagonia. GSA Bulletin 116, 308–321.

Kaplan, M.R., Douglass, D.C., Singer, B.S., Ackert, R.P., Caffee, M.W., 2005. Cosmogenic nuclide chronology of pre-last glacial maximum moraines at Lago Buenos Aires, 46°S, Argentina. Quat. Res. 63, 301–315.

Kaplan, M.R., Coronato, A., Hulton, N.R.J., Rabassa, J.O., Kubik, P.W., Freeman, S., 2007. Cosmogenic nuclide measurements in southernmost South America and implications for landscape change. Geomorphology 87, 284–301.

Kaplan, M.R., Fogwill, C.J., Sugden, D.E., Hulton, N.R.J., Kubik, P.W., Freeman, S.P.H.T., 2008. Southern patagonian glacial chronology for the last glacial period and implications for southern ocean climate. Quat. Sci. Rev. 27, 284–294.

Kaplan, M.R., Strelin, J.A., Schaefer, J.M., Denton, G.H., Finkel, R.C., Schwartz, R., Putnam, A.E., Vandergoes, M.J., Goehring, B.M., Travis, S.G., 2011. In-situ cosmogenic ^{10}Be production rate at Lago Argentino, Patagonia: implications for late-glacial climate chronology. Earth Planet Sci. Lett. 309, 21–32.

Kemp, R.A., McDaniel, P., Busacca, A.J., 1998. Genesis and relationship of macromorphology and micromorphology to contemporary hydrological conditions of a welded Argixeroll from the Palouse in Idaho. Geoderma 83, 309–329.

Kondo, R., Childs, C., Atkinson, I., 1994. Opal Phytoliths of New Zealand. Manaaki Whenua Press, Lincoln, Canterbury, p. 85.

Lal, D., 1991. Cosmic ray labeling of erosion surfaces: in-situ nuclide production rates and erosion models. Earth Planet Sci. Lett. 104, 424–439.

Lambert, F., Delmonte, B., Petit, J.R., Bigler, M., Kaufmann, P.R., Hutterli, M.A., Stocker, T.F., Ruth, U., Steffensen, J.P., Maggi, V., 2008. Dust-climate couplings over the past 800,000 years from the EPICA Dome C ice core. Nature 452, 616–619.

Leonard, G.S., Begg, J.G., Wilson, C.J.N., 2010. Geology of the Rotorua Area: Scale 1: 250,000 (compilers). Institute of Geological & Nuclear Sciences Limited. Institute of Geological & Nuclear Sciences 1:250,000 geological map 5, Lower Hutt, p. 99. + 1 folded map.

Litchfield, N.J., Reiser, U., 2005. Optically stimulated luminescence age constraints for fluvial aggradation terraces and loess in the eastern North Island, New Zealand. New Zealand Journal of Geology and Geophysics 48, 581–589.

Litchfield, N.J., Berryman, K.R., 2005. Correlation of fluvial terraces within the Hikurangi Margin, New Zealand: implications for climate and baselevel controls. Geomorphology 68, 291–313.

Lisiecki, L.E., Raymo, M.E., 2005. A Pliocene-Pleistocene stack of 57 globally distributed benthic δ^{18}O records. Paleoceanography 20, PA1003. https://doi.org/10.1029/2004PA001071.

Lowe, D.J., Tonkin, P.J., 2010. Unravelling upbuilding pedogenesis in tephra and loess sequences in New Zealand using tephrochronology. Proceedings, IUSS 19th World Congress of Soil Science, Brisbane. In: Proc. IUSS World Soil Congress Symposium 1.3.2 Geochronological Techniques and Soil Formation, Brisbane, August 1-6, 2010, pp. 34–37. Published on DVD and at. http://www.iuss.org.

Lowe, D.J., Palmer, D.J., 2005. Andisols of New Zealand and Australia. Journal of Integrated Field Science 2, 39–65.

Lowe, D.J., Tonkin, P.J., Palmer, J., Lanigan, K., Palmer, A.S., 2015. Dusty horizons. In: Graham, I. (Ed.), A Continent on the Move: New Zealand Geoscience Revealed, Second Edition, second ed., vol. 141. Geoscience Society of New Zealand with GNS Science, Lower Hutt, pp. 286–289.

Luzio, W., Casanova, M., Seguel, O., 2010. In: Luzio, W. (Ed.), Soils of Chile. University of Chile. Maval Press, Santiago (in Spanish).

McCulloch, R.D., Fogwill, C.J., Sugden, D., Bentley, M.J., Kubik, P.W., 2005. Chronology of the last glaciation in central strait of Magellan and Bahía inútil, southernmost south America: *Geografiska annaler*. Series A-Physical Geography 87, 289–312.

McDaniel, P.A., Lowe, D.J., Arnalds, O., Ping, C.-L., 2012. Andisols. Properties and Processes. In: Huang, P.M., Li, Y., Sumner, M.E. (Eds.), Handbook of Soil Sciences, second ed., vol. 1. CRC Press (Taylor & Francis), Boca Raton, Florida, pp. 33.29–33.48.

McDonald, E.V., Busacca, A.J., 1990. Interaction between aggrading geomorphic surfaces and the formation of a late Pleistocene paleosol in the Palouse loess of eastern Washington state. Geomorphology 3, 449–470.

McKeague, J.A., Day, J.H., 1966. Dithionite and oxalate-extractable Fe and Al as aids in differentiating various classes of soils. Can. J. Soil Sci. 46, 13–22.

Marx, S.K., McGowan, H.A., 2005. Dust transportation and deposition in a super-humid environment, West Coast, South Island, New Zealand. Catena 59, 147–171.

Massaferro, J., Larocque-Tobler, I., Brooks, S.J., Vandergoes, M., Dieffenbacher-Krall, A., Moreno, P.I., 2014. Quantifying climate change in Huelmo mire (Chile, Northwestern Patagonia) during the Last Glacial Termination using a newly

developed chironomid-based temperature model. Palaeogeogr. Palaeoclimatol. Palaeoecol. 399, 214—224.

Mercer, J.H., 1976. Glacial history of southern-most South America. Quat. Res. 6, 125—166.

Moar, N.T., 1980. Late otiran and early aranuian grassland in central South Island. New Zealand Journal of Ecology 3, 4—12.

Moreno, P.I., Leon, A.L., 2003. Abrupt vegetation changes during the last glacial to Holocene transition in mid-latitude South America. J. Quat. Sci. 18, 787—800.

Moreno, P.I., Videla, J., 2016. Centennial and millennial-scale hydroclimate changes in northwestern Patagonia since 16,000 yr BP. Quat. Sci. Rev. 149, 326—337.

Moreno, P.I., Denton, G.H., Moreno, H., Lowell, T.V., Putnam, A.E., Kaplan, M.R., 2015. Radiocarbon chronology of the last glacial maximum and its termination in northwestern Patagonia. Quat. Sci. Rev. 122, 233—249.

Nathan, S., Rattenbury, M.S., Suggate, R.P., (compilers), 2002. Geology of the Greymouth area: scale 1:250,000. Lower Hutt: Institute of Geological & Nuclear Sciences. Institute of Geological & Nuclear Sciences, 1:250,000 geological map 12, 58 p. + 1 folded map.

Nikiforoff, C.C., 1949. Weathering and soil evolution. Soil Sci. 67, 219—230.

Palmer, A.S., 1982c. Kawakawa tephra in wairarapa, New Zealand, and its use for correlating ohakea loess. New Zealand Journal of Geology and Geophysics 25, 305—315.

Palmer, A.S., Pillans, B.J., 1996. Record of climatic fluctuations from ca. 500 ka loess deposits and paleosols near Wanganui, New Zealand. Quat. Int. 34—36, 155—162.

Parfitt, R.L., Clayden, B., 1991. Andisols — the development of a new order in Soil Taxonomy. Geoderma 49, 181—198.

Parfitt, R.L., Russell, M., Orbell, G.E., 1983. Weathering sequence of soils from volcanic ash involving allophane and halloysite. Geoderma 29, 41—57.

Pesce, O.H., Moreno, P.I., 2014. Vegetation, fire and climate change in central-east Isla Grande de Chiloé (43°S) since the Last Glacial Maximum, northwestern Patagonia. Quat. Sci. Rev. 90, 143—157.

Pillans, B., 1983. Upper Quaternary marine terrace chronology and deformation, South Taranaki, New Zealand. Geology 11, 292—297.

Pillans, B., 1988. Loess chronology in Wanganui basin, New Zealand. In: Eden, Furkert, A.A. (Eds.), Loess - its Distribution, Geology and Soils. Balkema Publishers, Rotterdam, pp. 175—192.

Pillans, B., 1990a. Pleistocene marine terraces in New Zealand: a review. New Zealand Journal of Geology and Geophysics 33, 219—231.

Pillans, B., 1990b. Vertical displacement rates on quaternary faults, Wanganui basin. New Zealand Journal of Geology and Geophysics 33, 271—275.

Pillans, B.J., 2017. Quaternary stratigraphy of whanganui basin—a globally significant archive. In: Shulmeister, J. (Ed.), Landscape and Quaternary Environmental Change in New Zealand, Atlantis Advances in Quaternary Science, vol. 3, pp. 141—170.

Pillans, B., McGlone, M., Palmer, A., Mildenhall, D., Alloway, B.V., Berger, G., 1993. The last glacial Maxima in central and southern North Island, New Zealand: a paleoenvironmental reconstruction using the Kawakawa tephra formation as a chronostratigraphic marker. Paleogeography, Paleoclimatology, Paleoecology 101, 283—304.

Pillans, B., Froggatt, P., Kohn, B.P., Berger, G., Walter, R.C., Duller, G., Alloway, B.V., Hesse, P., 1996. Multi-method dating comparison for mid-Pleistocene Rangitawa Tephra, New Zealand. Quat. Sci. Rev. 15, 641—653.

Pino, M., Moreno, K., Riedemann, M.P., 2002. La terraza del último interglacial e la costa de Valdivia: observaciones, interpretaciones y desafíos. In: International Symposium on Environmental Geology for Land-use Planning, Extended Abstracts, Puerto Varas, Chile, pp. 24—28.

Raeside, J.D., 1964. Loess deposits of the South Island, New Zealand, and soils formed on them. New Zealand Journal of Geology and Geophysics 7, 811—838.

Railsback, L.B., Gibbard, P.L., Head, M.J., Voarintsoa, N.R.G., Toucanne, S., 2015. An optimized scheme of lettered marine isotope substages for the last 1.0 million years, and the climatostratigraphic nature of isotope stages and substages. Quat. Sci. Rev. 111, 94—106.

Simonson, R.W., 1959. Modern concepts of soil genesis. Soil Sci. Soc. Am. Proc. 23, 152—156.

Singer, B.S., Ackert, R.P., Guillou, H., 2004. ^{40}Ar/^{19}Ar and K-Ar chronology of Pleistocene glaciations in Patagonia. Geol. Soc. Am. Bull. 116, 434—450.

Smedley, R.K., Glasser, N.F., Duller, G.A.T., 2016. Luminescence dating of glacial advances at Lago Buenos Aires (similar to 46 degrees S), Patagonia. Quat. Sci. Rev. 134, 59—73.

Soil Survey Staff, 2014. Keys to Soil Taxonomy, twelfth ed. USDA-Natural Resources Conservation Service, Washington, DC, p. 360.

Stone, J.O., 2000. Air pressure and cosmogenic isotope production. J. Geophys. Res. 105, 23753—23759.

Suggate, R.P., 1990. Late pliocene and quaternary glaciations of New Zealand. Quat. Sci. Rev. 9, 175—197.

Thorveny, N., Caracaillet, J., Moreno, E., Leduc, G., Nerini, D., 2004. Geomagnetic moment variation and paleomagnetic excursions since 400 kyr BP: a stacked record from sedimentary sequences of the Portuguese margin. Earth Planet Sci. Lett. 219, 377—396.

Tonkin, P.J., Runge, E.C.A., Ives, D.W., 1974. A study of latePleistocene loess deposits, South Canterbury, New Zealand: Part 2. Paleosols and their stratigraphic implications. Quat. Res. 4, 217—231.

Tonkin, P.J., Basher, L.R., 2001. Soil chronosequences in subalpine superhumid Cropp basin, western southern Alps, New Zealand. New Zealand Journal of Geology and Geophysics 44, 37—45.

Vandergoes, M.J., Hogg, A.G., Lowe, D.J., Newnham, R.M., Denton, G.H., Southon, J., Barrell, D.J., Wilson, C.J., McGlone, M.S., Allan, A.S., 2013. A revised age for the Kawakawa/Oruanui tephra, a key marker for the Last Glacial Maximum in New Zealand. Quat. Sci. Rev. 74, 195—201.

Watt, S.F.L., Pyle, D.M., Mather, T.A., Martin, R.S., Matthews, N.E., 2009. Fallout and distribution of volcanic ash over Argentina following the May 2008 explosive eruption of Chaitén, Chile. J. Geophys. Res. 114 https://doi.org/10.1029/2008JB006219. B04207.

Wilson, C.J.N., Gravley, D.M., Leonard, G.S., Rowland, J.V., 2009. Volcanism in the central Taupo Volcanic Zone, New Zealand: tempo, styles and controls. In: Thordarson, T., Self, S., Larsen, G., Rowland, S.K., Hoskuldsson, A. (Eds.), Studies in Volcanology: the Legacy of George Walker, vol. 2. Special Publications of IAVCEI (Geological Society, London), pp. 225—247.

Wilson, K., Litchfield, N., Berryman, K., Little, T., 2007. Distribution, age, and uplift patterns of Pleistocene marine terraces of the northern Raukumara Peninsula, North Island, New Zealand. NZ Journ. Geol. Geophys. 50, 181—191.

Zárate, M.A., 2003. Loess of southern south America. Quat. Sci. Rev. 22, 1987—2006.